Molecular and Functional Characterization of Novel TRP Receptor-activated Ca^{2+} Channels from Mouse Brain

Takaharu Okada

Doctor of Philosophy

Department of Physiological Sciences

School of Life Science

The Graduate University of Advanced Studies

1998

CONTENTS

INTRODUCTION

Calcium (Ca^{2+}) influx across the plasma membrane plays a vital role in the regulation of diverse cellular processes, ranging from ubiquitous activities like gene expression to tissue-specific functions such as neurotransmitter release and muscle contraction, by controlling the cytosolic free Ca^{2+} concentration ($[Ca^{2+}]_i$) (Tsien and Tsien, 1990; Clapham, 1995). Recently, in addition to the well characterized modes of Ca^{2+} entry through voltage-dependent Ca^{2+} channels and ligand-gated cation channels, receptor-activated Ca^{2+} influx that occurs as a second phase of phosphatidyl inositol (PI) - dependent response, has been recognized for its physiological significance (Fasolato et al., 1994). In the immune system, receptor-activated Ca^{2+} influx is necessary for sustained $[Ca^{2+}]_i$ rises in T- and B-lymphocytes which eventually cause proliferation and differentiation of lymphocytes (Gardner, 1989; Partiseti et al., 1994). In the nervous system, especially, the importance of the channels responsible for receptor-activated Ca^{2+} influx should consist in their ability not only to increase $[Ca^{2+}]_i$ but also to depolarize the membrane potential. In fact, excitatory postsynaptic potentials induced by stimulation of Gq-coupled metabotropic glutamate receptors were reported to appear at parallel fiber synapses on cerebellar Purkinje cells depending on the conditions of parallel fiber stimulation. This suggests these channels are involved in a kind of synaptic plasticity (Batchelor and Garthwaite, 1997).

Diverse ion channels activated by various triggers have been recognized to be responsible for the receptor-activated Ca^{2+} influx (Fasolato et al., 1994). Among the members of the group, recent attention was particularly directed to capacitative Ca^{2+} entry (CCE; in other words, Ca^{2+} release-activated current (I_{CRAC}), or store-operated channel (SOC)), that is activated through Ca^{2+} release from the intracellular Ca^{2+} store, endoplasmic reticulum (ER), induced by inositol 1,4,5-trisphosphate (IP_3) and

consequent depletion of Ca^{2+} from the store (Putney, 1990; Irvine, 1990; Putney and Bird, 1993; Fasolato et al. 1994; Partiseti et al., 1994; Serafini et al., 1995; Berridge, 1995; Clapham, 1995). Diffusible small molecules (Randriamampita and Tsien, 1993; Parekh et al., 1993), IP_3 metabolites (Parekh et al., 1997), and direct coupling of IP_3 receptors (IP_3R) or small GTP-binding (G) proteins with the channel proteins (Irvine, 1990; Putney and Bird, 1993; Berridge, 1995; Kiselyov et al., 1998) have been proposed to be involved in the activation of this Ca^{2+} entry pathway. Other plasma membrane ion channels directly activated by second messengers such as Ca^{2+}, IP_3, and inositol 1,3,4,5-tetraphosphate (IP_4) (Kuno and Gardner, 1987; Restrepo et al., 1990; Mozhayeva et al., 1991; Luckhoff and Clapham, 1992) are also categorized as receptor-activated Ca^{2+} channels (Fasolato et al. 1994).

An important clue for understanding the molecular basis of receptor-activated Ca^{2+} influx was first attained through the finding of a *Drosophila* visual transduction mutation *transient receptor potential* (*trp*), whose photoreceptors fail to generate the Ca^{2+}-dependent sustained phase of receptor potential and to induce subsequent Ca^{2+}-dependent adaptation to light (Fein et al., 1984; Ranganathan et al., 1995). Since the gene products of the *trp* and *trp-like* (*trpl*) gene (TRP and TRPL) comprise the light-activated, PI-dependent Ca^{2+} conductance in *Drosophila* photoreceptors (Niemeyer et al., 1996), the original hypothesis that the counterparts of TRP and TRPL are responsible for CCE in vertebrate cells, was based upon analogy between the phototransduction mechanism in *Drosophila* and the PI-dependent signal transduction processes in vertebrates (Ranganathan et al., 1995). In fact, recent molecular characterization has unveiled the existence of multiple genes encoding TRP homologues in vertebrate cells, and cDNAs encoding mammalian TRP homologues designated as TRP1 and TRP3 were cloned (Petersen et al., 1995; Wes et al., 1995; Zhu et al., 1995; Zitt et al., 1996; Zhu et al.,

1996). Recombinant expression experiments of *Drosophila* TRP and TRPL, and mammalian TRP1 and TRP3 present some lines of supportive evidence for the hypothesis that TRP and its homologues, except TRPL, are CCE channels (Vaca et al., 1994; Hu and Schilling, 1995; Petersen et al., 1995; Zitt et al., 1996; Zhu et al., 1996; Obukhov et al., 1996; Hardie et al., 1997; Xu et al., 1997; Preuß et al., 1997). However, the hypothesis is still controversial (Niemeyer et al., 1996; Clapham, 1996; Acharya et al., 1997). Acharya et al. (1997) demonstrated that photoreceptors from *Drosophila* with homozygous loss-of-function mutation of IP_3R were indistinguishable from wild-type controls in sensitivity, kinetics, and adaptation of response to light. Furthermore, most significantly, low IP_3 concentrations can induce substantial Ca^{2+} release from the stores without activating Ca^{2+} entry at all in rat basophilic leukemia cells, suggesting that even the activation of CCE is not that tightly coupled to Ca^{2+} release from the IP_3-sensitive stores (Parekh et al., 1997). Thus, criteria of activation trigger other than depletion of Ca^{2+} store, should be considered in functionally establishing cloned TRP channels to be correlated with native Ca^{2+} channels responsible for receptor-activated Ca^{2+} influx, including CCE.

I have here isolated cDNAs that encode novel TRP homologues, TRP4, TRP5, TRP6, and TRP7 from the mouse brain. All of these homologues were found to be relatively highly expressed in the brain, but their expression was detected also in various organs other than the brain, with various intensities characteristic of each subtype. Among them, first, I characterized the function of the brain-predominant homologue, TRP5. The recombinant expression of the TRP5 cDNA in human embryonic kidney (HEK) cells potentiated an extracellular Ca^{2+}-dependent increase of $[Ca^{2+}]_i$ evoked by ATP, but not by an inhibitor of ER Ca^{2+}-ATPases, thapsigargin. Whole-cell mode of patch-clamp recordings from TRP5-expressing cells demonstrated that ATP application

induced a large inward current in the presence of extracellular Ca^{2+}, which reversed at a positive potential. The TRP5 activity was abolished by omission of intracellular Ca^{2+} and by treatment with a calmodulin antagonist. High concentration of extracellular Ca^{2+} activated TRP5 without ATP stimulation. On the other hand, omission of extracellular Ca^{2+} abolished the activity even in the presence of ATP. These results suggest that TRP5 directs the formation of a highly Ca^{2+}-permeable ion channel which can be activated through receptor-operative pathways other than depletion of Ca^{2+} from Ca^{2+} stores, and that the activity of this channel is highly dependent on Ca^{2+} concentrations inside and outside of cells in the brain. Second, I also characterized the TRP7 function using the same recombinant expression system. The results show that TRP7 directs the formation of a Ca^{2+}-permeable ion channel with significant basal activity. The activity of TRP7 does not depend on extracellular Ca^{2+} and is enhanced by receptor-stimulation even with the low concentration of ATP which itself cannot induce Ca^{2+} release from the intracellular Ca^{2+} store. The obtained functional characters of the two novel TRP homologues together suggest that mammalian TRP homologues are members of a large family of channels responsible for receptor-activated Ca^{2+} influx including not only SOC but also other diverse subtypes of channels in the family.

EXPERIMENTAL PROCEDURES

cDNA cloning and Sequence Determination

A mixture of oligo(dT)-primed cDNAs synthesized from the mouse (BALB/c or 129/SvJ) brain poly(A)$^+$ RNA was subjected to PCR amplification using the Marathon cDNA Amplification kit (Clontech, Palo Alto, CA). Degenerate oligonucleotide primers (5'-TGGGGCC(T/C/A)(T/C)TGCAGAT(A/C)TC(T/A)CTGGGA-3' and 5'-(G/T)G(A/T)TCG(A/G)GCAAA(C/T)TTCCA(C/T)TC-3') were designed according to the conserved amino acid sequence between *Drosophila* TRP and TRPL. Obtained PCR products were subsequently subcloned into the T/A cloning plasmid, pCRII (Invitrogen, Carlsbad, CA) to yield p1054, pTRP15 and pTRP16. Sequence comparison with PCR products amplified using pairs of specific oligonucleotide primers TK30 (5'-GCAGATATCTCTGGGAAG-3') and TK32 (5'-TTTGTTCGAGCAAATTTCC-3'), T5-1 (5'-TATCTACTGCCTAGTACTACTGG-3') and T5-2 (5'-GCAATGAGCTGGTAGGAGTTATTC-3'), and T6-1 (5'-ATCGGCTACGTTCTGTATGGTGTC-3') and T6-2 (5'-GGAAAACCACAATTTGGCCCTTGC-3') according to the partial genomic nucleotide sequence given in Zhu et al. (1996) confirmed that the cDNA inserts carried by p1054, pTRP15 and pTRP16 encode mouse TRP4, TRP5 and TRP6, respectively.

Further screening was performed to obtain entire coding cDNAs for mouse TRP4, TRP5 and TRP6. Oligo(dT)-primed, size-selected (>1 kilobase pairs (kb)) cDNA libraries constructed in the λ Uni-ZAP XR vector (Stratagene, La Jolla, CA) using poly(A)$^+$ RNA from the brain of adult BALB/c or postnatal 14 day-old (P14) C57BL/6J mice were screened to yield TRP4 clones λh1 (1835-3179; nucleotide numbers from the first residue of the initiation ATG triplet), λh5 (1729-3443), and λO3 (-124 to 3237 followed by a poly(dA) tract), TRP5 clones λm37 (1020-3166) and λO4 (1134-3287

followed by a poly(dA) tract), and TRP6 clones λm2 (461-2971) and λm44 (1126-2971 followed by a poly(dA) tract).

Additional clones harboring cDNAs for the further upstream regions of mouse TRP5 were isolated by screening a specific oligonucleotide-primed cDNA transcripts of poly(A)$^+$ RNA from the brain of P14 C57BL/6J mice constructed in the λ Uni-ZAP XR vector. The specific oligonucleotide primer (5'-GAGAGAGAGAGAGAGAGAACTAGTCTCGAGTCAAGCAGCATTCGTCCC-3') was designed according to the sequence in the clone λm37 and designed to contain an additional sequence of a *Xho*I site protected by GA repeats for subcloning into the λ Uni-ZAP XR vector. λO15 (-232 to 1547) and other thirteen hybridization positive clones were isolated through hybridization with the 657-base pair (bp) *Eco*RI(on vector)/*Bam*HI(1665) fragment from λm37.

To obtain the further upstream region of the TRP6 cDNA, rapid amplification of 5'-cDNA ends (5'-RACE) was performed using the Marathon cDNA Amplification Kit (Clontech, Palo Alto, CA) according to the manufacturers instructions with minor modifications. The template cDNAs were constructed from P14 C57BL/6J (B6) mouse brain poly(A)$^+$ RNA. The PCR amplification was performed using Advantage cDNA PCR Kit (Clontech, Palo Alto, CA). The sequences of specific primers used were 5'-ATGCTGGACTTGCCAGACCTTTGTATGC-3'. The resulting ~0.7-kb cDNA fragment were subcloned into pBluescript SK(+) (Stratagene) to yield a clone p5RACE6 (-118 to 850).

To search for a novel mouse TRP homologue, library screening was performed using the cDNA encoding mouse TRP2 as a probe. The TRP2 cDNA fragment was obtained by PCR amplification from a mixture of oligo(dT)-primed cDNAs synthesized from the mouse (BALB/c or 129/SvJ) brain poly(A)$^+$ RNA using Marathon cDNA

Amplification kit (Clontech, Palo Alto, CA). A pair of specific oligonucleotide primers used were T2-1 (5'-GACGACATGATCCGGTTCATGTTC-3') and T2-2 (5'-CTCGATCTTCTGGAAGGAGTTGGTG-3') according to the partial genomic nucleotide sequence given in Zhu et al. (1996). Screening with low stringency the oligo(dT)-primed, size-selected (>1 kb) adult mouse (129/SvJ or BALB/c) brain cDNA library constructed in the Uni-ZAP XR vector (Stratagene) yielded a clone λa11. Sequence comparison with the known mammalian TRP homologues (TRP1-6) revealed that λa11 carried the cDNA (-94 to 2071) of the novel TRP homologue designated TRP7. To obtain the entire coding mouse TRP7 cDNA, rapid amplification of 3'-cDNA ends (3'-RACE) was performed using the Marathon cDNA Amplification kit (Clontech). The specific primer used was T7-7 (5'-CGTGCTGTATGGGGTTTATAATGTCACC-3'). The template cDNAs and the conditions were as described above for 5'-RACE of TRP6. The resulting ~1.2-kb cDNA fragments were subcloned into pBluescript SK(+) (Stratagene) to a yield clone pRACE7 (1950-3085 followed by a poly(dA) tract). Through comparison with other TRP homologues, it was suggested that the region of cDNA (781-1128) was absent in λa11 due to alternative splicing. The region was amplified by RT-PCR from adult mouse brain total RNA using AMV reverse transcriptase and LA-Taq DNA polymerase (Takara) and the specific primers (5'-GACTACTTCTGCAAGTGCAATGAGTGC-3' and 5'-TTCCACAAGTGTAGCACGTACTCCC-3') according to the manufacturers instructions. The resulting 0.25~0.7-kb cDNA fragments were subcloned into pGEM-T Easy vector (Promega) to yield p7α, p7β, p7γ, and p7δ carrying the ~0.70, ~0.52, ~0.33, and ~0.25-kb spliced variants, respectively, of TRP7 cDNA. The insert of p7γ corresponded to the spliced form of cDNA carried by λa11.

cDNA clones were sequenced on both strands using an automated sequencer (Perkin Elmer model 373S; Perkin Elmer, Foster City, CA).

Northern Blot Analysis

RNA blot hybridization analysis was carried out using 20 μg of total RNA from various tissues. The probes for detection of mouse TRP1was the ~0.4-kb mouse TRP1 cDNA fragment amplified using Marathon cDNA Amplification Kit (Clontech). and the specific primers (5'-GGAACTTACAATGTTGTGGTT-3' and 5'-CTTACAATATGCTGTCATTC-3') synthesized according to the nucleotide sequences in Sakura and Ashcroft (1997). For mouse TRP3, TRP4, TRP5, TRP6, and TRP7, the ~1.9-kb *Eco*RI/*Eco*RI fragment from the mouse TRP3 clone λm9 (Mori et al., 1998), the ~1.3-kb *Eco*RI/*Eco*RI fragment from λh1, the ~0.9-kb *Eco*RI/*Hin*dIII fragment from λO4, the ~0.8-kb *Eco*RI/*Hin*dIII fragment from λm44, and the ~0.44-kb *Sac*I/*Pvu*II fragment from p3RACE7, respectively. Random Primer DNA Labeling Kit Ver.2 (Takara, Otsu, Japan) was used to prepare the ^{32}P-labeled probes. Hybridization was performed at 42 ℃ in 50 % formamide, 5 × SSC, 50 mM sodium phosphate buffer (pH 7.0), 0.1 % SDS, 0.1 % polyvinylpyrrolidone, 0.1 % Ficoll 400 (Pharmacia Biotech, Uppsala, Sweden), 0.1 % bovine serum albumin, and 0.2 mg/ml sonicated herring sperm DNA, as described previously (Mori et al., 1991).

Reverse Transcriptase (RT)-PCR Amplification and Southern Blot Analysis

Reverse transcription and PCR amplification from 1 μg total RNA were performed using rTth DNA polymerase (RT-PCR high -Plus-; TOYOBO, Osaka, Japan). Pairs of primers used for amplification of TRP5 and cyclophilin were T5-1 and T5-2 (see above), and 5'-GCAGCCATGGTCAACCCCACCG-3' and 5'-

GAAATTAGAGCTGTCCACAGTCGG-3' (accession No. X52803), respectively. The thermocycler was programmed to give an initial cycle consisting of 60 ℃ reverse transcription for 5 min and 94 ℃ denaturation for 2 min followed by 40 cycles of 94 ℃ denaturation for 1 min and 52 ℃ annealing / extention for 1.5 min. The final cycle was followed by an additional extention at 52 ℃ for 7 min. To verify the identity of the PCR products, Southern blots were hybridized with ^{32}P-5' end-labeled synthetic oligonucleotide probes 5'-ATGAACCTAACAACTGCAAGG-3' and 5'-CGACATCACGGCCGATGACGAGCCC-3' for detection of TRP5 and cyclophilin mRNAs, respectively. Hybridization was performed at 50 ℃ in 6 × SSC, 50 mM sodium phosphate buffer (pH 7.0), 0.2 % SDS, 0.1 % polyvinylpyrrolidone, 0.1 % Ficoll 400, 0.1 % bovine serum albumin, and 0.1 mg/ml sonicated herring sperm DNA.

Recombinant Expression in HEK Cells

A PCR product amplified from the clone λO15 using a sense primer (5'-GGGTCGACGGGTTTTTATTTTTAATTTTCTTTCAAATACTTCCACCATGGCCCAGCTGTACTAC-3'), designed to contain the untranslated leader (UTL) sequence from the alfalfa mosaic virus (Jobling and Gehrke, 1987), a consensus sequence for translation initiation (Kozak, 1986), and nucleotide residues 1-18 of TRP5, and an antisense primer (5'-CCAAAGGATCCATGCAGTTGATGTTGAC-3') was digested with *Sal*I and *Bam*HI. Another PCR product amplified from λO4 using a sense primer (5'-CCTCTGCAGATCTCTTTGGGACGAATGC-3') and an antisense primer (5'-ATGGCGGCCGCAAAACATGAAGAATGTGGC-3') was digested with *Pst*I and *Not*I. The resulting fragments were ligated with the *Bam*HI(199)/*Pst*I(1521) fragment from λO15 and the 5.5-kb *Sal*I/*Not*I fragment from pCI-neo (Promega, Madison, WI) to yield pCI-neo-mTRP5.

The DNA constructs for recombinant expression of TRP7 were prepared as

described below. A PCR product amplified from the clone λa11 using a sense primer (5'-GGGTCGACGGGTTTTTATTTTTAATTTTCTTTCAAATACTTCC ACCATGTTGGGGAGCAACACC-3') and an antisense primer (5'-AGTGACCTCCAAGTGCTC-3') was digested with *Sal*I and *Apa*LI. Another PCR product amplified from pRACE7 using the specific primer used for TRP7 3'-RACE as a sense primer and an antisense primer (5'-ATGCGGCCGCTTTGGAATGCTGTTAGAC-3') was digested with *Nco*I and *Not*I. The resulting fragments were ligated with one of the *Apa*LI(701)/*Nco*I(1999) fragments from p7α, p7β and p7γ, and the 5.5-kb *Sal*I/*Not*I fragment from pCI-neo (Promega, Madison, WI) to yield pCI-neo-mTRP7α, pCI-neo-mTRP7β and pCI-neo-mTRP7γ, respectively. The plasmid pCI-neo-mTRP3 for TRP3 expression were also constructed in the similar way using the clones described in Mori et al. (1998).

HEK293 cells (RIKEN Cell Bank, Tsukuba, Japan) were transfected with one of the plasmids for recombinant expression of mouse TRP homologues plus πH3-CD8 containing the cDNA of the T-cell antigen CD8 (Jurman et al., 1994). Transfection was carried out using SuperFect Transfection Reagent (QIAGEN, Hilden, Germany). Cells were trypsinized, diluted with Dulbecco's modified Eagle's medium (DMEM) containing 10 % fetal bovine serum (FBS), 30 units/ml penicillin, and 30 μg/ml streptomycin, and plated onto glass coverslips 18 h after transfection. Then cells were subjected to measurements 36-66 h after plating on the coverslips. TRP homologue-expressing cells were selected through detection of CD8 coexpression using polystyrene microspheres precoated with antibody to CD8 (Dynabeads M-450 CD8; DYNAL, Oslo, Norway).

Measurement of Changes in $[Ca^{2+}]_i$

Cells on coverslips were loaded with fura-2 by incubation in DMEM containing 5 μM fura-2/AM (Dojindo Laboratories, Kumamoto, Japan) and 10 % FBS at 37 ℃ for 30 min, and washed with the HEPES-buffered saline (HBS) containing (in mM): 107 NaCl, 6 KCl, 1.2 $MgSO_4$, 2 $CaCl_2$, 1.2 KH_2PO_4, 11.5 glucose, 20 HEPES, adjusted to pH 7.4 with NaOH. The coverslips were then placed in a perfusion chamber mounted on the stage of the microscope. Fluorescence images of the cells were recorded and analyzed with a video image analysis system (ARGUS-50/CA, Hamamatsu Photonics, Hamamatsu, Japan) according to the method of Hazama and Okada (1990). The fura-2 fluorescence at an emission wavelength of 510 nm (bandwidth, 20 nm) was observed at room temperature by exciting fura-2 alternatingly at 340 and 380 nm (bandwidth, 11 nm). The 340/380 nm ratio images were obtained on a pixel by pixel basis, and were converted to Ca^{2+} concentrations by *in vitro* calibration. The calibration procedure was performed according to Ueda and Okada (1989). All the reagents dissolved in water or dimethylsulfoxide were diluted to their final concentrations in HBS or Ca^{2+}-free HBS containing (in mM): 107 NaCl, 6 KCl, 1.2 $MgSO_4$, 1.2 KH_2PO_4, 0.5 EGTA, 11.5 glucose, 20 HEPES, adjusted to pH 7.4 with NaOH, and applied to the cells by perfusion. $LaCl_3$ and $GdCl_3$ (100 mM in water) were diluted in HBS or Ca^{2+}-free HBS from which KH_2PO_4 was omitted. Data were accumulated under each condition from 2 - 4 experiments using cells prepared through 2 - 3 transfections.

Measurement of Mn^{2+} influx

Fluorescence quenching was studied using the fura-2 isosbestic excitation wavelength at 360 nm and recording emitted fluorescence at 510 nm with the same system as used in $[Ca^{2+}]_i$ measurement. The fluorescence intensity relative to the initial values were obtained on a pixel by pixel basis. $MnCl_2$ and ATP dissolved in water were diluted to their final concentrations in nominally Ca^{2+}-free HBS or HBS containing 0.1 mM or 1

mM Ca^{2+}.

Electrophysiology

For electrophysiological measurements, coverslips with cells were placed in dishes containing the solutions. Cells prepared in this manner had membrane capacitance of 21.3 ± 2.3 pF (n = 25). Currents from cells were recorded at room temperature using patch-clamp techniques of whole-cell mode (Hamill et al., 1981) with an EPC-7 patch-clamp amplifier (List-Medical, Darmstadt, Germany). Patch pipettes were made from borosilicate glass capillaries (1.5 mm outer diameter; Hilgenberg, Malsfeld, Germany) using a model P-87 Flaming-Brown micropipette puller (Sutter Instrument, San Rafael, CA). Pipette resistance ranged from 2 to 4 MΩ when filled with the pipette solution described below. Currents were sampled at 200 Hz after low-pass filtered at 1 kHz (-3dB) using an 8-pole Bessle filter (900, Frequency Devices, Haverhill, MA) for Fig. 7, *a* and *b*, sampled at 1 kHz for Fig. 7*c*, and analyzed with pCLAMP 6.02 software (Axon Instruments, Foster City, CA). The pipette solution for Fig. 7 contained (in mM): CsOH 105, aspartic acid 105, CsCl 40, $MgCl_2$ 2, $CaCl_2$ 3.2, EGTA 5, Na_2ATP 2, HEPES 5, adjusted to pH7.2 with CsOH. Calculated free Ca^{2+} concentration was 200 nM. When $CaCl_2$ was 1.33 and 0.34 mM in the pipette solution, calculated free Ca^{2+} concentration was 50 and 10 nM, respectively. The "0Ca^{2+}" external solution contained (in mM): NaCl 140, $MgCl_2$ 1.2, $CaCl_2$ 1.2, EGTA 10, glucose 10, HEPES 11.5, adjusted to pH 7.4 with NaOH (8 nM calculated free Ca^{2+}). The "10Ca^{2+}" external solution contained (in mM): NaCl 122.4, $MgCl_2$ 1.2, $CaCl_2$ 10, glucose 30, HEPES 11.5, adjusted to pH 7.4 with NaOH. The osmolarity of the external solutions was adjusted to about 325 mOSM. Rapid exchange of the external solutions was made by a modified "Y-tube" method (Nakagawa et al., 1990).

RESULTS

Primary structures of the TRP homologues

It was very important to clone vertebrate TRP homologues because it was the only way to access molecular entity of channels responsible for receptor-activated Ca^{2+} influx in vertebrate cells. As for mammalian TRP homologues, cDNA cloning of human TRP1 and TRP3 had been reported (Wes et al., 1995; Zhu et al., 1995; Zitt et al., 1996; Zhu et al., 1996). Here I isolated cDNAs of the four novel mammalian TRP homologues, TRP4, TRP5, TRP6, and TRP7 from the mouse brain (see EXPERIMENTAL PROCEDURES). Figure 1A shows the alignment of the amino acid sequences of the four mouse TRP proteins deduced from the open reading frames of the corresponding cDNA sequences. TRP4, TRP5, TRP6, and TRP7 are composed of 974, 975, 930, and 862 amino acid residues, respectively. The amino acid sequences 781-864 in TRP4, and 322-376 and 261-376 in TRP7 (corresponding to the clones p7β and p7γ, respectively, described above in Experimental Procedures) can be lost through altanative RNA splicing. Translation of TRP7 can be terminated at the 322nd amino acid residue changed from phenylalanine to glutamate because of the frame shift also through alternative RNA splicing (corresponding to the clone p7δ).

Hydropathy profile revealed that all of them had eight hydrophobic segments and hydrophilic N and C termini (Fig. 1B), similar to those of other TRP subtypes (Montell and Rubin, 1989; Phillips et al., 1992; Wes et al., 1995; Zhu et al., 1995; Zitt et al., 1996; Zhu et al., 1996; Philipp et al., 1996). Sufficient length of hydrophobic regions to span the membrane, together with the lack of a hydrophoic N-terminal sequence indicative of the signal sequence, suggests that they are membrane protein with a core of transmembrane segments and the flanking N- and C-terminal regions disposed on the cytoplasmic side, like other TRP subtypes (Montell and Rubin, 1989; Phillips et al., 1992; Wes et al., 1995; Zhu et al., 1995; Zhu et al., 1996; Philipp et al., 1996). The following lines of indication favor a transmembrane topology model comprised of six

rather than eight transmembrane regions (Fig. 1C). The fourth (H4), fifth (H5) through sixth (H6), and eighth (H8) hydrophobic regions display homology to the third, fourth through fifth, and sixth putative transmembrane segments, respectively, of the *Drosophila* PARA Na^+ channel (Mori et al., 1998). Thus, the two short hydrophobic regions H3 and H7 may partly span the membrane as a hairpin and contribute to forming the pore wall structure of the TRP channels as seen in voltage-gated channels.

Fig. 1D depicts the phylogenetic tree of the TRP family constructed by the neighbor-joining method (Saitou and Nei, 1987), based on the sequence alignment carried out by the Clustal w program (Thompson et al., 1994). A cloned vanilloid receptor (rVR1), a non-selective cation channel involved in pain pathways which was reported to be structurally related to members of the TRP family (Caterina et al., 1997) is also included in Fig. 1C. According to the tree mammalian TRP homologues are broadly divided into the three groups, one containing TRP1, one containing TRP3, TRP6 and TRP7, and one containing TRP4 and TRP5. Sequence identity/similarity is 66.9/78.6 % between two of mouse TRP4 and TRP5, 69.2-80.6/80.0-89.2 % between two of mouse TRP3, TRP6 and TRP7, 33.7-80.6/55.1-89.2 % between two of all mouse TRP homologues, 31.6-36.9/51.9-56.3 % between one of mammalian TRP homologues and one of Drosophila TRP and TRPL, and 11.9-14.7/32.2-37.6 % between one of all TRP subtypes and rVR1. Homology of the TRP family members is relatively localized in the N-terminal region and the hydrophobic core.

Tissue distribution of the mammalian TRP homologues

RNA preparation from mouse tissues were subjected to Northern blot analyses using cDNAs of TRP1, TRP3, TRP4, TRP5, TRP6 and TRP7 as specific probes to reveal their tissue distribution (Fig. 2, A~F). Although all the homologues were detected to be expressed in the brain, the data indicate their differential distribution in the tissues inside and outside of the brain.

The ~4.0 kb TRP3 mRNA was highly expressed in the cerebellum, but it was weakly expressed in the cerebrum (Fig. 2C). By contrast, the major ~3.7 kb species and the minor ~7.0 kb and ~2.2 kb species of TRP4 mRNA were found predominantly in the cerebrum, which were marginally detectable to be expressed in the cerebellum (Fig. 2D). The differential distribution of TRP3 and TRP4 mRNAs was confirmed by the experiment using the in-situ hybridization techniques, which revealed that TRP3 and TRP4 mRNAs were concentrated in the cerebellar Purkinje cell layer and the hippocampal CA1 region, respectively (Mori et al., 1998). Expression at low levels was detected also in the heart and lung for TRP3, and in the uterus for TRP4 (Fig. 2, C and D).

For TRP1, TRP6, and TRP7, the highest expression was not detected in the brain, but in the tissues outside of the brain. The ~4.0 kb and ~1.7 kb species of TRP6 mRNA are most abundant in the lung, and at the lower level in the spleen. In the brain, expression of TRP6 mRNA is higher in the forebrain region (olfactory bulb, cerebrum, and midbrain) than in the hindbrain region (cerebellum and medulla-pons). The ~1.7 kb specie of TRP6 mRNA is the major in the brain, and only the weak signals of this specie were detected in the heart and uterus. TRP1 and TRP7 are distributed similarly, being expressed strongly in the heart and lung, and relatively weakly in the brain, spleen and kidney (Fig. 2, A and B). For TRP1 and TRP7, the signal at the size of ~4.0 kb and the smeared signal at the larger sizes were detected.

Distinct from the other mouse TRP homologues, TRP5 mRNA was exclusively detected in the brain by the Northern analysis (Fig. 2E). An intense signal of TRP5 mRNA with the size of ~8.5 kb was present in the forebrain region and a relatively weak signal was detected in the hindbrain region. To detect trace levels of TRP5 mRNA expression in the tissues other than the brain, a pair of primers was designed to amplify cDNA sequences within the TRP5 cDNA probe used in the Northern analysis. As shown in Figure 2G, RT-PCR amplification for 40 cycles, which is beyond the exponential phase of amplification, and subsequent Southern blot hybridization using a

TRP5-specific oligonucleotide probe disclosed TRP5 expression not only in the brain regions, but also in liver, kidney, testis, and uterus (Garcia and Schilling, 1997). In addition to the main hybridizable PCR product, ~330 bp, which corresponds to the expected size, a second hybridizable product of ~250 bp was detected in the hindbrain region, liver, kidney, testis, and uterus, but not in the forebrain.

Functional characterization of TRP5: cytosolic Ca^{2+} measurements

Next, I did the experiments to elucidate functional properties of the cloned TRP homologues. Among the homologues, first, I selected the almost brain-specific TRP5 to characterize, about which even the amino acid sequences had not been reported. HEK293 cells are capable of serving as an excellent expression system for studying functional properties of TRP5 as a receptor-activated Ca^{2+} channel, since they express the P_2 purinoceptor coupled to activation of G_q protein and phospholipase C (Bischof et al., 1997). HEK cells were also reported for the absence of endogenous TRP5 expression (Garcia and Schilling, 1997). TRP5 together with a marker protein CD8 was transiently expressed in HEK cells, and intracellular Ca^{2+} concentration was monitored in transfectants and non-transfected control HEK cells using fura-2 as an indicator.

In the presence of 2 mM extracellular Ca^{2+}, application of 100 μM ATP to control cells induced a rapid rise in $[Ca^{2+}]_i$ that peaked within 30 s and gradually decreased to the resting level within 300 s (Fig. 3A). This transient rise in $[Ca^{2+}]_i$ was presumed to be mainly due to release from the intracellular Ca^{2+} store, since omission of extracellular Ca^{2+} affected little on the peak level (Fig. 4A), whereas the decay phase was accelerated in the absence of extracellular Ca^{2+}. When 100 μM ATP was applied to TRP5-transfected, CD8-positive cells in the presence of extracellular Ca^{2+}, the peak

$[Ca^{2+}]_i$ level greatly increased (Fig. 3B). In TRP5-expressing cells, Ca^{2+} influx across the plasma membrane was a major cause of the $[Ca^{2+}]_i$ rise, since the amplitude of $[Ca^{2+}]_i$ rise was much smaller in the absence of extracellular Ca^{2+} than that in the presence of extracellular Ca^{2+} at ATP concentrations above 1 μM (Fig. 3C), and remained almost the same as that of $[Ca^{2+}]_i$ transient evoked in control cells in the absence of extracellular Ca^{2+} (Fig. 4, A and B). $[Ca^{2+}]_i$ rise evoked by ATP in TRP5-expressing cells in the presence and absence of extracellular Ca^{2+}, and in control cells in the presence of extracellular Ca^{2+} increased in a similar dose-dependent manner (Fig. 3C).

To separate contribution to $[Ca^{2+}]_i$ rise of Ca^{2+} influx from that of Ca^{2+} release, ATP was first applied in the absence of extracellular Ca^{2+}, and 2 mM Ca^{2+} was then added to the extracellular solution when $[Ca^{2+}]_i$ returned to the resting level (3 min after addition of ATP). Addition of Ca^{2+} to the extracellular solution only slightly raised $[Ca^{2+}]_i$ above the resting level in control cells (Fig. 4, A and C), whereas in TRP5-transfected cells, it elicited dramatic $[Ca^{2+}]_i$ transients (Fig. 4, B and C) which reached maximum in the presence of ATP ≥ 10 μM (Fig. 4C). The second $[Ca^{2+}]_i$ rise evoked by extracellular Ca^{2+} did not seem to correlate with the preceding first $[Ca^{2+}]_i$ rise caused by ATP-dependent Ca^{2+} release from the intracellular Ca^{2+} store. The second $[Ca^{2+}]_i$ rise was 613 ± 77 (mean ± SEM) nM for the TRP5-expressing cells that showed the first rise staying below 10 nM (n = 16), and was not significantly different from that (452 ± 40 nM) observed in the cells where the first rise was above 10 nM (n = 48). Time-lag between start of ATP stimulation and addition of extracellular Ca^{2+} did not significantly affect amplitude of $[Ca^{2+}]_i$ rise up to 5 min (Fig. 4D). Interestingly, after 3 min

stimulation by ATP in Ca^{2+}-free solution, thapsigargin induced intact $[Ca^{2+}]_i$ rises in untransfected cells (102 ± 4 nM, n = 53), as compared to control cells without ATP stimulation (113 ± 5 nM, n = 51) (see below). Furthermore, after initial application of ATP for 3 min and subsequent omission of ATP up to 5 min in Ca^{2+}-free solution, untransfected cells did not show significant $[Ca^{2+}]_i$ rise induced by the second application of ATP (n = 38). These results suggest that ATP receptors are rapidly desensitized by incubating with 100 μM ATP, and thereby internal stores are replenished with Ca^{2+} within 3 min. Without ATP, $[Ca^{2+}]_i$ rise was not observed in TRP5-transfected cells that were immersed in the Ca^{2+}-containing solution after preincubation in the Ca^{2+}-free solution for up to 7 min (data not shown).

Lanthanides, La^{3+} and Gd^{3+}, were reported to block currents induced by recombinant expression of *Drosophila* TRP, TRPL, human TRP1, TRP3 (Zitt et al., 1996; Zhu et al., 1996; Sinkins et al., 1996), and Ca^{2+} channels characterized in native preparations (Boland et al., 1991; Lacampagne et al., 1994; Chang et al., 1995) and I_{CRAC} (Hoth and Penner, 1993). The imidazol derivative, SK&F96365, inhibits various types of ion channels including receptor-activated channels (Clementi and Meldolesi, 1996; Waldron et al., 1997). In Fig. 5, 100 μM ATP was added alone (Fig. 5A) or together with one of the agents (25 μM SK&F96365 (Fig. 5B) or 100 μM La^{3+} (Fig. 5C)) to the Ca^{2+}-free extracellular solution, and 2 mM Ca^{2+} was further added 3 min later. As shown in Fig. 5B, C and D, 25 μM SK&F96365 and 100 μM La^{3+} significantly suppressed the second $[Ca^{2+}]_i$ increase due to Ca^{2+} influx. However, compared to the two agents, the effect of 100 μM Gd^{3+} on the amplitude of the second $[Ca^{2+}]_i$ rise was not as significant (Fig. 5D). These results indicate that ATP-induced Ca^{2+} influx in

TRP5-transfected cells is sensitive to blockade by SK&F96365 and La^{3+} (Fig. 5D).

To examine whether the $[Ca^{2+}]_i$ transient due to TRP5-mediated Ca^{2+} influx is activated by depletion of the intracellular Ca^{2+} store induced by IP_3-dependent Ca^{2+} release via phospholipase C stimulation, we used, instead of ATP, the specific inhibitor of sarcoplasmic and endoplasmic reticulum ATPases (SERCAs), thapsigargin (Inesi and Sagara, 1994). As the cells were perfused with Ca^{2+}-free solution containing 2 μM thapsigargin, $[Ca^{2+}]_i$ was transiently increased and thereafter reduced to the basal level (Fig. 6, A and B). Subsequent addition of Ca^{2+} (2 mM) to the extracellular solution transiently increased $[Ca^{2+}]_i$ in TRP5-transfected cells (Fig. 6B) to the level similar to that in control cells (Fig. 6A), indicating that CCE is not potentiated by expression of TRP5. This observation suggests that TRP5 is not activated by store depletion.

We further tested whether ATP is capable of activating Ca^{2+} influx in the TRP5-expressing cells where thapsigargin-induced Ca^{2+} influx is already activated. When cells were perfused with the solution containing 2 mM Ca^{2+} and 2 μM thapsigargin, transient $[Ca^{2+}]_i$ increase developed similarly in the control and transfected cells, decreasing within 1000 s after addition of thapsigargin to stationary levels that stayed slightly above the initial basal levels (Fig. 6, C and D). Replacement of thapsigargin with 100 μM ATP transiently increased $[Ca^{2+}]_i$ without any latency in TRP5-transfected cells (Fig. 6D), whereas it slightly decreased $[Ca^{2+}]_i$ in control cells (Fig. 6C). The results overall indicate that ATP activates Ca^{2+} influx by a trigger different from depletion of the Ca^{2+} store.

Functional characterization of TRP5 – electrophysiological measurements

To directly demonstrate that TRP5 is responsible for Ca^{2+} influx activated by ATP in HEK cells, ionic currents triggered by ATP stimulation in TRP5-transfected cells were characterized in comparison with those in control non-transfected HEK cells, using whole-cell mode of patch-clamp. When 200 nM free Ca^{2+} was present in the patch pipette, and ATP was added to the "0Ca^{2+}" external solution, 16 out of 18 CD8-positive, TRP5-transfected HEK cells showed inward currents accompanied with an increase in the amplitude of current fluctuation (Fig. 7B). Rapid exchange of the "0Ca^{2+}" external solution with the "10Ca^{2+}" external solution induced a rapid development of large inward currents, followed by a gradual increase of inward currents in 7 out of the 16 cells (Fig. 7B). The remaining 9 cells did not show further increase of currents by the solution change. The augmentation of the inward current was abolished quickly upon the removal of Ca^{2+}, although the fluctuation of currents remained until ATP was washed out. In the control cells (n = 7), 100 μM ATP did not induce significant ionic currents regardless of the presence of 10 mM Ca^{2+} in extracellular solution (Fig. 7A). When Ca^{2+} concentration in pipette solution was reduced to 50 nM, similar proportion of the CD8-positive, TRP5-transfected cells (11 out of 12 cells) showed responsiveness to ATP. However, usage of 10 nM free Ca^{2+} intrapipette solution resulted in slightly reduced number of the CD8-positive, TRP5-transfected HEK cells responsive to ATP, inducing inward currents in 6 out of 9 cells. The CD8-positive, TRP5-transfected HEK cells measured using the EGTA-containing, Ca^{2+}-free pipette solution were not responsive to ATP (n = 5).

Current-voltage relationship of ionic current triggered by ATP in TRP5-expressing cells was examined using negative voltage ramps from 40 to -70 mV for 1.5 s. Five consecutive voltage ramps were applied . The averages of current traces generated by 5 consecutive ramps every 5 s in the "0Ca^{2+}" external solution and the "10Ca^{2+}"

external solution with 100 μM ATP were drawn in Fig. 7C. The current-voltage relationship recorded in "10Ca^{2+}" was non-linear, showing a significant inward current at physiological potentials. Permeability ratios among Na^+, Cs^+, and Ca^{2+} were estimated on the basis of the Goldman-Hodgkin-Katz equation using the reversal potentials in Fig. 7C. On the assumption that activity coefficients are 0.3 for Ca^{2+} and 0.75 for both Na^+ and Cs^+, the reversal potentials of 8 mV in the "0Ca^{2+}" external solution and 17 mV in the "10Ca^{2+}" solution lead to permeability ratios $P_{Ca} : P_{Na} : P_{Cs}$ = 14.3 : 1.5 : 1.

Pharmacological study on the mechanisms of intracellular Ca^{2+} involvement in TRP5 activation

As described above, whole-cell inward currents in ATP-stimulated, TRP5-transfected cells using the pipette solution containing free Ca^{2+} exhibited rapid and dramatic increases upon addition of Ca^{2+} to the extracellular solution, whereas those measured using the EGTA-containing, Ca^{2+}-free pipette solution were not responsive to ATP. These data imply an important role of intracellular Ca^{2+} in activation of TRP5. Ca^{2+}-binding proteins such as calmodulin and Ca^{2+}-dependent kinases are possible mediators for the effect of intracellular Ca^{2+} on the TRP5 acitvity. First, the involvement of calmodulin was investigated using the inhibitor of calmodulin, W-13 (Hidaka and Tanaka, 1983). Besides TRP5-transfected cells, here TRP3-transfected cells were also used for the experiments, because TRP3 has been reported to form a nonselective cation channel that is activatable by the increase of $[Ca^{2+}]_i$ (Zitt et al., 1997). $[Ca^{2+}]_i$ in TRP5- and TRP3-transfected cells was measured using the protocol similar to one described in Fig. 4 in the presence of W-13 at various concentration. As shown in Fig. 8, A~D, W-13 inhibited ATP-induced Ca^{2+} influx via both TRP5 and TRP3 at the concentration ranges corresponding to the range at which the drug inhibits a number of calmodulin activities

(Fujinaga et al. 1994).

Next, two inhibitors for myosin light chain kinase, a Ca^{2+}/calmodulin-dependent kinase, were tested for inhibition of the activities of TRP5 and TRP3. The inhibitors, wortmannin (Nakanishi et al., 1992; Watanabe et al., 1996) and ML-9 (Watanabe et al., 1996), inhibited Ca^{2+} influx via TRP5 at the adequate concentration range (Fig. 9, A, B, C, and D). However the TRP3 activity was insensitive to wortmannin, and was less sensitive to ML-9 than TRP5 although it was inhibited at concentrations higher than 3 μM (Fig. 9, E, F, G, and H). I also tested the effect of KN-93, a inhibitor of Ca^{2+}/calmodulin-dependent kinase II (CAMKII) which is another Ca^{2+}/calmodulin-dependent kinase, and its derivative KN-92 ineffective for the CAMKII activity (Peretz et al., 1998). Although KN-93 inhibited both the TRP5 and TRP3 activity (to 33 % and 30 % at 10 μM, respectively), KN-92, which should have been a negative control, inhibited the TRP5 and TRP3 activity (to 24 % and 25 % at 10 μM, respectively) rather more effectively than KN-93.

Involvement of extracellular Ca^{2+} in TRP5 activation

As shown in Fig. 10, $[Ca^{2+}]_i$ in individual ATP-stimulated, TRP5-expressing cells rose with various duration of latency after the addition of extracellular Ca^{2+}, whereas those $[Ca^{2+}]_i$ rises in individual TRP3-expressing cells synchronized. This suggests a important role of extracellular Ca^{2+} in inducing the TRP5 activity. Furthermore, when the ion permeation properties through the TRP5 channel was investigated by electrophysiological experiments using the extracellular solution containing various concentrations of Ca^{2+}, it was found that extracellular Ca^{2+} (>= 5 mM) elicited the TRP5-dependent large inward current without ATP stimulation (Wakamori et al., unpublished data). This was confirmed by $[Ca^{2+}]_i$ measurement. TRP5-transfected cells were exposed to 2, 5, 10, 15, or 20 mM extracellular Ca^{2+} after 3-min incubation in the EGTA-

containing Ca^{2+}-free solution. Figure 11, A~E show the representative traces of changing $[Ca^{2+}]_i$ in individual cells. Two millimolar extracellular Ca^{2+} hardly elicited $[Ca^{2+}]_i$ rises (Fig. 11A). Significant $[Ca^{2+}]_i$ rises were observed in a small population of the cells (4 in 23 cells used for measurement) with some duration of latency after the addition of 5 mM extracellular Ca^{2+} (Fig. 11B). As extracellular Ca^{2+} concentration applied was increased over 5 mM, the amplitude of $[Ca^{2+}]_i$ rises (Fig. 11F) and the population of the cells showing $[Ca^{2+}]_i$ rises (10 mM; 7 in 18 cells, 15 mM; 15 in 28 cells, and 20 mM; 19 in 22 cells) increased and the duration of latency became shorter (Fig. 11, C~E).

Next, the effect of extracellular Ca^{2+} on the TRP5 activity in the presence of ATP was tested. The TRP5 activity was observed by measuring the quenching of $[Ca^{2+}]_i$-independent fluorescence caused by Mn^{2+} influx, instead of the $[Ca^{2+}]_i$-dependent change in fluorescence spectrum. This method has the advantage that the effect of the change in extracellular Ca^{2+} concentration on the TRP5 activity can be estimated relatively independently of the effect on the driving force for Ca^{2+} to permeate the channel, at least when extracellular Ca^{2+} concentration is not high compared to Mn^{2+} concentration. When TRP5-transfected cells were stimulated with 100 μM ATP in the solutions containing 100 μM Mn^{2+} and various concentrations of Ca^{2+} (nominally free, 0.1 mM, and 1 mM), the extent of fluorescence quenching increased as extracellular Ca^{2+} concentration applied was increased as shown in Fig. 12A. In the nominally Ca^{2+} free solution there was no significant quenching induced by ATP stimulation. On the contrary, in the case of TRP3-transfected cells ,Mn^{2+} influx induced by ATP was most significant in the nominally Ca^{2+}-free solution, and blocked by extracellular Ca^{2+} dose-dependently (Fig. 12B). This blockade is thought to caused by the competition between Ca^{2+} and Mn^{2+} for the channel pore. This should be also the case with TRP5, and the TRP5 activity in the presence of 1 mM extracellular Ca^{2+} is probably underestimated compared to the activity in the presence of 0.1 mM Ca^{2+} from the data shown in Fig. 12A.

In fact, in the presence of 2 mM Ca^{2+}, the extent of fluorescence quenching induced by ATP was smaller than in the presence of 1 mM Ca^{2+} (data not shown).

Functional Characterization of TRP7

I investigated the functional properties of TRP7 also, about which even the existence has not been reported. TRP7α together with a marker protein CD8, or CD8 alone was transiently expressed in HEK cells, and intracellular Ca^{2+} concentration was monitored using fura-2 as an indicator. In the presence of 2 mM extracellular Ca^{2+}, application of 100 μM ATP to control CD8-positive cells induced a rapid rise in $[Ca^{2+}]_i$ that peaked within 20 s and gradually decreased to the resting level within 300 s (Fig. 13A). As described above about non-transfected cells in Fig. 3, this transient rise in $[Ca^{2+}]_i$ was presumed to be mainly due to release from the intracellular Ca^{2+} store, because omission of extracellular Ca^{2+} did not significantly affected on the peak level (Fig. 13B), whereas the decay phase was accelerated in the absence of extracellular Ca^{2+}. When 100 μM ATP was applied to TRP7α-transfected, CD8-positive cells in the presence of extracellular Ca^{2+}, the $[Ca^{2+}]_i$ increase in the cells was larger and sustained much longer than in control cells. The $[Ca^{2+}]_i$ level did not decrease completely to the resting level even 30 min after the start of ATP stimulation (data not shown). In TRP7α-expressing cells, Ca^{2+} influx across the plasma membrane was likely to be a major cause of the $[Ca^{2+}]_i$ rise, because in the absence of extracellular Ca^{2+} the $[Ca^{2+}]_i$ increase was very transient (Fig. 13C) and much smaller than in the presence of extracellular Ca^{2+} at ATP concentration above 0.1 μM (Fig. 13B). Interestingly, this $[Ca^{2+}]_i$ increase due to ATP-induced Ca^{2+} release from the internal Ca^{2+} store was smaller in TRP7α-expressing cells than in control cells (Fig. 13B and C).

The ATP-induced Ca^{2+} influx in TRP7α-expressing cells was observed in the isolated form by the experiment shown in Fig. 13C. ATP was first applied in the absence of extracellular Ca^{2+}, and 2 mM Ca^{2+} was then added to the extracellular solution when $[Ca^{2+}]_i$ returned to the level before ATP application. Addition of Ca^{2+} to the extracellular solution only slightly raised $[Ca^{2+}]_i$ above the resting level in control cells, whereas in TRP7α-transfected cells, it elicited the large and sustained $[Ca^{2+}]_i$ rise. Importantly, ATP concentration required to enhance the extracellular Ca^{2+}-dependent $[Ca^{2+}]_i$ rise in TRP7α-expressing cells was obviously lower than that needed to induce Ca^{2+} release from the intracellular Ca^{2+} store: 1 μM ATP was almost sufficient to induce TRP7α-dependent Ca^{2+} influx maximally, but hardly elicited Ca^{2+} release from the store (Fig. 13B and D). This indicates that activation of TRP7α is not coupled to Ca^{2+} release from the intracellular Ca^{2+} store or consequent depletion of the Ca^{2+} store as well as TRP5 activation described above.

Furthermore TRP7α had the significant activity without any stimulation by agonists like ATP. In the presence of extracellular Ca^{2+}, the resting $[Ca^{2+}]_i$ level in TRP7α-expressing cells was higher than in control cells (Fig. 13A and C). After Ca^{2+} was removed from the external solution, $[Ca^{2+}]_i$ in TRP7α-expressing cells fell to the level as in control cells (Fig. 13C). Re-addition of 2 mM extracellular Ca^{2+} raised $[Ca^{2+}]_i$ back to the level at which it had been before the Ca^{2+} removal. This significant agonist-independent activity seems to be one of the characters which make TRP7α distinct from other mammalian TRP homologues. This was not observed in measuring $[Ca^{2+}]_i$ in the cells functionally expressing TRP5 and TRP3. Although TRP3 which is the most homologous subtype of TRP7 was also reported to have some basal activities (Zhu et al.,

1998), these activities of TRP3 appear to be low compared to those of TRP7α. In the presence of 1 mM Mn^{2+} in the nominally Ca^{2+}-free external solution, basal Mn^{2+} influx was observed much more significantly in TRP7α-transfected cells than in TRP3-transfected cells (Fig. 14A), whereas TRP7α and TRP3 introduced Mn^{2+} into the cells to the similar degrees when they were maximally activated by 100 μM ATP (Fig. 14B).

I have as well examined the cells transfected with TRP7β and TRP7γ also, which are the alternatively spliced forms of TRP7. However, basal and ATP receptor stimulation-induced Ca^{2+} influx in these transfectants were not significantly different from vector-transfected cells, although Ca^{2+}-release from the intracellular Ca^{2+} store seemed to be a little reduced by expression of TRP7β and TRP7γ in the manner similar to that in TRP7α-transfected cells (data not shown).

DISCUSSION

Activation mechanism of TRP5 essential for receptor-activated Ca^{2+} influx

In the present investigation, I have cloned and functionally characterized the mouse TRP homologue, designated as TRP5, predominantly expressed in the brain. Recombinant expression of the TRP5 cDNA in HEK cells potentiated transient increases in $[Ca^{2+}]_i$ evoked by ATP in the presence of extracellular Ca^{2+} (Fig. 3). When Ca^{2+} was added to the extracellular solution after preincubating the cells in the Ca^{2+}-free solution under constant ATP stimulation, potentiation of transient $[Ca^{2+}]_i$ rise induced by TRP5 expression became more prominent (Fig. 4). In this experiment, the second $[Ca^{2+}]_i$ rise due to Ca^{2+} influx showed no significant correlation with the first $[Ca^{2+}]_i$ rise due to Ca^{2+} release from IP_3-sensitive internal stores in the absence of extracellular Ca^{2+}. In extreme cases, $[Ca^{2+}]_i$ rise through Ca^{2+} influx was induced in a TRP5-expressing cell where Ca^{2+} release was hardly detectable. When thapsigargin was substituted for ATP to deplete the internal Ca^{2+} store by inhibiting ER Ca^{2+}-ATPases, the second $[Ca^{2+}]_i$ rise due to CCE was not potentiated by TRP5 expression (Fig. 6, A and B). These results indicate that TRP5 is responsible for Ca^{2+} influx activated by ATP via mechanisms other than Ca^{2+} depletion from the internal Ca^{2+} store.

Independence of TRP5-activating cascades from depletion of the internal Ca^{2+} stores is confirmed by additional lines of experimental evidence. In the presence of extracellular Ca^{2+}, after the thapsigargin-induced $[Ca^{2+}]_i$ transient decayed to a plateau level, another $[Ca^{2+}]_i$ rise was induced in TRP5-expressing cells by ATP (Fig. 6D), which did not induce $[Ca^{2+}]_i$ transients but even elicited slight decreases of $[Ca^{2+}]_i$ in control cells (Fig. 6C). The lack of ATP-induced Ca^{2+} release from ER in control cells

after thapsigargin treatment (Fig. 6C) indicates that the ATP-sensitive stores are included in the thapsigargin-sensitive stores, excluding the possibility that TRP5 is activated via depletion of the ATP-sensitive stores independent of the thapsigargin-sensitive stores. It is also unlikely from this finding that TRP5 activation is directly coupled with the Ca^{2+}-releasing process involving the IP_3Rs. Furthermore, the results indicate that after 3-min stimulation by ATP in Ca^{2+}-free solution, TRP5 channels are still activable (Fig. 4B) but endogenous receptor-activated channels including CCE channels, whose activation by thapsigargin is clearly seen in Fig. 6A, are dormant in HEK cells (Fig. 4A). This is presumably due to difference between the TRP5 channel and endogenous channels in susceptibility to effects of ATP receptor desensitization. Desensitization of ATP receptors within 3 min is suggested from the experimental observation that in Ca^{2+}-free solution, $[Ca^{2+}]_i$ transient was not any more induced by ATP after initial application of ATP for 3 min and subsequent washing out of ATP for 5 min. Rapid desensitization of ATP receptors, compared to other types of receptors, was also reported by other groups (Bischof et al., 1997). After 3-min application of ATP in Ca^{2+}-free solution, $[Ca^{2+}]_i$ rise induced by subsequent application of thapsigargin was intact, suggesting that internal stores were rapidly replenished with Ca^{2+}. Thus, after desensitization of ATP receptors and replenishment of Ca^{2+} stores, activation signals for TRP5 channel still persist, while activation trigger for CCE is already abolished.

From the experiments, some insights can be gained into the activation mechanism for TRP5. Present data imply an important role of intracellular Ca^{2+} in activation of TRP5. Whole-cell inward currents in ATP-stimulated, TRP5-transfected cells measured using the pipette solution containing free Ca^{2+} exhibited rapid and dramatic increases upon addition of Ca^{2+} to the extracellular solution (Fig. 7B), whereas those which measured using the EGTA-containing, Ca^{2+}-free pipette solution were not

responsive to ATP. $[Ca^{2+}]_i$ could be lowered to 10 nM, that is considerably lower than physiological $[Ca^{2+}]_i$, to elicit TRP5 current in HEK cells, whereas higher percentage of the TRP5 current-positive cells was obtained when $[Ca^{2+}]_i$ was elevated to 50 nM and 200 nM. This observation suggests that TRP5 is activatable in the physiological range of $[Ca^{2+}]_i$ even at basal levels. Ca^{2+} may acts through Ca^{2+}-binding proteins such as calmodulin and Ca^{2+}-dependent enzymes. This proposal is supported by the data which showed that the calmodulin antagonist W-13 inhibited ATP-induced Ca^{2+} entry into TRP5-expressing cells (Fig. 8, A and B). How Ca^{2+}/calmodulin is involved in TRP5 activation, however, is still unclear. Although involvement of a Ca^{2+}/calmodulin-dependent kinase, MLCK, is suggested by the data from the pharmacological experiments (Fig. 9, A, B, E, and F), there are a number of possible mechanisms including the binding of the kinase to TRP5 or other proteins, and/or subsequent phosphorylation.

In thapsigargin-treated, TRP5-expressing cells, ATP primed the activity of TRP5 presumably not through $[Ca^{2+}]_i$ elevation (Fig. 6D), since the action of ATP on $[Ca^{2+}]_i$ was toward decrease from slightly elevated levels in thapsigargin-treated control cells (Fig. 6C). This excludes the possibility that Ca^{2+} is a sole activation trigger for TRP5, strongly suggesting involvement of other factors in TRP5 activation. It is possible that slight decrease from the elevated level (in the presence of thapsigargin) optimizes $[Ca^{2+}]_i$ in the range that activates but does not inactivate TRP5. Activation of Gq protein, phospholipase Cβ, and protein kinase C, and production of phosphoinositide metabolites such as IP_3 and IP_4, which are all triggered by stimulation of ATP receptors, should be considered as candidate activators of TRP5.

On the other hand, extracellular Ca^{2+} could behave solely as a activation trigger for TRP5 (Fig. 11). There are three possible sites where Ca^{2+} added to the external solution attacks to activate TRP5: some endogeously expressed Ca^{2+}-binding protein

protruding extracellularly like Ca^{2+}-sensing receptors, TRP5 itself, and intracellular Ca^{2+}-binding proteins. If the first possibility was the case, there should be the reason why the TRP3 activity was insensitive to extracellular Ca^{2+} (Fig. 11). The most attractive reason would be that there are some combinations of metabotropic receptors and receptor-activated channels which are preferably coupled, for example Ca^{2+}-sensing receptors and TRP5 in this case. If the second was true, there would be binding sites for Ca^{2+} in this protein. If the third was the case, there should be some entrance for Ca^{2+} into the cell. The entrance might be TRP5 itself in a mode with low opening probability. And even though the third one was true, it would not be sole sites to be attacked by Ca^{2+} because intracellular Ca^{2+} cannot be a sole activation trigger as described above. No matter which is true, the resulting conclusion can be of interest.

Obtained results are also indicative of a role of Ca^{2+} as a negative regulator for TRP5. In the presence of extracellular Ca^{2+}, $[Ca^{2+}]_i$ transients induced by ATP stimulation decreased almost to the basal level (Fig. 3B) at the time when the second $[Ca^{2+}]_i$ rise induced by Ca^{2+} addition with time lag of 3 min after ATP stimulation reached peak (Fig. 4B). Negative regulatory action of Ca^{2+} has been reported for *Drosophila* TRP, TRPL (Xu et al., 1997), and CCE in *Xenopus* oocytes (Petersen and Berridge, 1994).

Human TRP3 has been reported to form a non-selective cation channel that is not sensitive to Ca^{2+} store depletion (Zitt et al., 1997; Zhu et al., 1998). Specifically, Zitt et al. (1997) have shown that Ca^{2+} neither act alone or act together with calmodulin directly on the TRP3 protein to activate the channel. During the present investigation in progress, it was reported that mouse TRP6 encodes a non-selective cation channel stimulated by the muscarinic M5 receptor, but not by intracellular store depletion (Boulay et al., 1997). And here I showed that mouse TRP7 can also be activated to introduce Ca^{2+} into the cell by receptor stimulation which does not cause Ca^{2+} release from the store

(Fig. 13B). It is therefore possible that the Ca^{2+}-selective TRP5 channels are activated via common activation mechanisms which operate in opening the TRP3 channel, the TRP6 channel and/or the TRP7 channel.

Functional diversity of TRP homologues and correlation with native receptor-activated Ca^{2+} channels

It has been hypothesized that TRP homologues encode channels responsible for CCE or ICRAC in vertebrate cells. Here I showed the functional properties of the novel mouse homologues, TRP5 and TRP7 using the recombinant expression system, and concluded both of them encode channels activated by receptor-operative pathways other than Ca^{2+} release from the Ca^{2+} store and subsequent depletion of the store. The TRP6 activity was also reported to be independent of the store-operated pathways (Boulay et al., 1997). However there are other mammalian TRP homologues, TRP1, TRP3, and TRP4 reported to function as store-operated channels, although experimental criteria to determine whether store-operated or not in those reports may be incomplete (Zitt et al., 1996; Zhu et al., 1996; Philipp et al., 1996). In addtion, TRP3 is thought to have activities dependent on receptor stimulation but independent of store-operative pathways, and these activities are the major compared with the store-dependent activity (Zhu et al., 1998).

Besides receptor-operated pathways to activation, TRP homologues are diverse also in other functional properties. Ca^{2+} influx via TRP5 activated by receptor stimulation is often very transient, whereas Ca^{2+} influxes via TRP3 and TRP7 are sustained much longer in the presence of the agonist (Fig. 10). In addition, there are some homologues like TRP7 which have high basal activities and causes significant extracellular Ca^{2+}-dependent $[Ca^{2+}]_i$ increases without any receptor-stimulation or other treatment, and other homologues with low basal activities like TRP5. Permeation properties can be also diverse. The whole-cell current measurements using patch pipettes filled with the solution containing 200 nM free Ca^{2+} demonstrated that rapid

exchange of the external "0Ca^{2+}" solution with the "10Ca^{2+}" solution elicited instantaneous and dramatic increases of inward TRP5 currents (Fig. 7B), which reversed at positive potentials (Fig. 7C). This, together with the permeability ratios (P_{Ca} : P_{Na} : P_{Cs} = 14.3 : 1.5 : 1) calculated from the reversal potentials, indicates that TRP5 is selective for Ca^{2+} over monovalent cations. Of the other recombinantly expressed TRP homologues, *Drosophila* TRP and mammalian TRP4 were demonstrated for Ca^{2+} selectivity (Vaca et al., 1994; Philipp et al., 1996; Xu et al., 1997), while *Drosophila* TRPL, and mammalian TRP1, TRP3 and TRP6 were rather classified as non-selective cation channels (Hu et al., 1995; Zitt et al., 1996; Zitt et al., 1997; Birnbaumer et al., 1996; Xu et al., 1997).

Although a considerable amount of knowledge about functional properties of TRP homologues has been accumulated as described above, functional correspondence between cloned TRP homologues and Ca^{2+} channels responsible for receptor-activated Ca^{2+} influx, including CCE, in native preparations is still very controversial. Ca^{2+} selectivity in permeation has been one of the important criteria in correlating recombinant TRP homologues with native Ca^{2+} channels (Clapham, 1996). In the native systems, the TRP and TRPL components of light-activated current isolated through usage of *trpl* and *trp* mutant photoreceptors showed ion selectivity comparable with those of the recombinant TRP and TRPL (Niemeyer et al., 1996; Hardie and Minke, 1992). Among the receptor-activated Ca^{2+} channels in vertebrate cells, known for diversity in ion permeation properties (Fasolato et al., 1994), some display ion selectivity that may correspond well to TRP homologues. However, establishing functional correlation of TRP with native receptor-activated Ca^{2+} channels becomes considerably unsuccessful by introduction of activation trigger as a second distinguishing criterion. Although I_{CRAC} has selectivity for Ca^{2+} over Na^{+}, Ba^{2+}, and Mn^{2+} as TRP5 does (Hoth and Penner,

1992; wakamori et al., unpulished data), and is regulated positively and negatively by extracellular Ca^{2+} as TRP5 is, depletion of the intracellular Ca^{2+} store does not activate TRP5, but activates the nonselective cation channels TRP1 (Zitt et al., 1996), TRP3 (Birnbaumer et al., 1996). Another putative store-operated channel TRP4 does not have Ca^{2+} selectivity comparable to I_{CRAC}, and other properties of this homologue characterized so far is too poor to be correlated with those of native channels from other points of view. In contrast to TRP5, IP_4 and Ca^{2+}-sensitive channels in endothelial cells are not only highly permeable to Ca^{2+}, but also to other divalent cations such as Ba^{2+} and Mn^{2+} (Luckhoff and Clapham, 1992). It has also been reported that Ba^{2+} or monovalent cations are as permeant as Ca^{2+} in other receptor-activated Ca^{2+} channels triggered by second messengers such as IP_3 or by activation of G-proteins (Fasolato et al., 1994). Thus, each vertebrate TRP homologue expressed in heterologous systems do not really correspond to the native receptor-activated Ca^{2+} channels in both the two functional criteria, activation trigger and Ca^{2+} selectivity.

Heteromultimer formation by multiple TRP isoforms (Xu et al., 1997) may be necessary to elicit native type receptor-activated Ca^{2+} entry. In present expression studies of TRP5, there was no clear functional indication for presence of heterogeneous populations of heteromultimer and homomultimer, although Garcia and Schilling (1997) have shown endogenous expression of TRP1, TRP3, TRP4, and TRP6 mRNAs in HEK 293 cells. This may derive from the usage of ATP receptor stimulation in activating Ca^{2+} entry, or low mRNA expression levels of endogenous TRP isoforms compared to the level of TRP5 overexpression. It would be necessary to characterize functional properties of neuronal receptor-activated Ca^{2+} channels at exact expression sites of individual TRP homologues determined by *in situ* hybridization (Funayama et al., 1996; Mori et al., 1998) and immunohistochemistry in native tissues, and to compare them with

those of recombinant receptor-activated channels composed of appropriate TRP combinations. For example, expression TRP3 and TRP7 was detected in cerebellar Purkinje cells by *in situ* hybridization (Mori et al., 1998), and it is very interesting to verify whether they are responsible for the metebotropic glutamate receptor-dependent EPSP at parallel fiber synapses on Purkinje cells using techniques of electrophysiology and molecular biology (Batchelor and Garthwaite, 1997).

REFERENCES

Acharya, J. K., Jalink, K., Hardy, R. W., Hartenstein, V., and Zuker, C. S. (1997). $InsP_3$ receptor is essential for growth and differentiation but not for vision in Drosophila. *Neuron* **18**, 881-887

Batchelor, A.M., and Garthwaite, J. (1997). Frequency detection and temporally dispersed synaptic signal association through a metabotropic glutamate receptor pathway. *Nature* **385**, 74-77.

Berridge, M. J. (1995). Capacitative calcium entry. *Biochem. J.* **312**, 1-11

Birnbaumer, L., Zhu, X., Jiang, M., Boulay, G., Peyton, M., Vannier, B., Brown, D., Platano, D., Sadeghi, H., Stefani, E., and Birnbaumer, M. (1996). On the molecular basis and regulation of cellular capacitative calcium entry: roles for Trp proteins. *Proc. Natl. Acad. Sci. USA* **93**, 15195-15202

Bischof, G., Serwold, T. F., and Machen, T. E. (1997). Does nitric oxide regulate capacitative Ca influx in HEK 293 cells? *Cell Calcium* **21**, 135-142

Boland, L. M., Brown, T. A., and Dinglendine, R. (1991). Gadolinium block of calcium channels: influence of bicarbonate. *Brain Res.* **563**, 142-150

Boulay, G., Zhu, X., Peyton, M., Jiang, M., Hurst, R., Stefani, E., and Birnbaumer, L. (1997). Cloning and expression of a novel mammalian homolog of Drosophila transient receptor potential (Trp) involved in calcium entry secondary to activation of receptors coupled by the Gq class of G protein. *J. Biol. Chem.* **272**, 29672-29680

Caterina, M. J., Schumacher, M. A., Tominaga, M., Rosen, T. A., Levine, J. D., Julius, D. (1997). The capsaicin receptor: a heat-activated ion channel in the pain pathway. *Nature* **389**, 816-824

Chang, A. S., Chang, S. M., Garcia, R. L., and Schilling, W. P. (1997). Concomitant and hormonally regulated expression of trp genes in bovine aortic endothelial cells. *FEBS Lett.* **415**, 335-340

Chang, W., Chen, T. H., Gardner, P., and Shoback, D. (1995). Regulation of Ca^{2+}-conducting currents in parathyroid cells by extracellular Ca^{2+} and channel blockers. *Am. J. Physiol.* **269**, E864-E877

Clapham, D. E. (1995). Calcium signaling. *Cell* **80**, 259-268

Clapham, D. E. (1996). TRP is cracked but is CRAC TRP? *Neuron* **16**, 1069-1072

Clementi, E., and Meldolesi, J. (1996). Pharmacological and functional properties of voltage-independent Ca^{2+} channels. *Cell Calcium* **19**, 269-279

Fasolato, C., Innocenti, B., and Pozzan, T. (1994). Receptor-activated Ca^{2+} influx: how many mechanisms for how many channels? *Trends Pharmacol. Sci.* **15**, 77- 83

Fein, A., Payne, R., Corson, D. W., Berridge, M. J., and Irvine, R. F. (1984). Photoreceptor excitation and adaptation by inositol 1,4,5-trisphosphate. *Nature* **311**, 157-160

Fujinaga, M., Hoffman, B. B., Baden, J. M. (1994). Receptor subtype and intracellular signal transduction pathway associated with situs inversus induced by alpha 1 adrenergic stimulation in rat embryos. *Dev Biol.* **162**, 558-567

Funayama, M., Goto, K., and Kondo, H. (1996). Cloning and expression localization of cDNA for rat homolog of TRP protein, a possible store-operated calcium (Ca^{2+}) channel. *Mol. Brain Res.* **43**, 259-266

Garcia, R. L., and Schilling, W. P. (1997). Differential expression of mammalian TRP homologues across tissues and cell lines. *Biochem. Biophys. Res. Commun.* **239**, 279-283

Gardner, P. (1989). Calcium and T lymphocyte activation. *Cell* **59**, 15-20

Hamill, O. P., Marty, A., Neher, E., Sakmann, B., and Sigworth, F. J. (1981). Improved patch-clamp techniques for high-resolution current recording from cells and cell-free membrane patches. *Pflügers Arch. - Eur. J. Physiol.* **391**, 85-100

Hardie, R. C., and Minke, B. (1992). The trp gene is essential for a light-activated Ca^{2+} channel in Drosophila photoreceptors. *Neuron* **8**, 643-651

Hardie, R. C., Reuss, H., Lansdell, S. J., and Millar, N. S. (1997). Functional equivalence of native light-sensitive channels in the Drosophila trp301 mutant and TRPL cation channels expressed in a stably transfected Drosophila cell line. *Cell Calcium* **21**, 431-440

Hazama, A., and Okada, Y. (1990). Biphasic rises in cytosolic free Ca^{2+} in association with activation of K^+ and Cl^- conductance during the regulatory volume decrease in cultured human epithelial cells. *Pflügers Arch. - Eur. J. Physiol.* **416**, 710-714

Hidaka, H., and Tanaka, T. (1983). Naphthalenesulfonamides as calmodulin antagonists. *Methods Enzymol.* **102**, 185-194

Hoth, M., and Penner, R. (1992). Depletion of intracellular calcium stores activates a calcium current in mast cells. *Nature* **355**, 353-356

Hoth, M, and Penner, R. (1993). Calcium release-activated calcium current in rat mast cells. *J. Physiol.* **465**, 359-386

Hu, Y., and Schilling, W. P. (1995). Receptor-mediated activation of recombinant Trpl expressed in Sf9 insect cells. *Biochem. J.* **305**, 605-611

Inesi, G., and Sagara, Y. (1994). Specific inhibitors of intracellular Ca^{2+} transport ATPases. *J. Membrane Biol.* **141**, 1-6

Irvine, R. F. (1990). 'Quantal' Ca^{2+} release and the control of Ca^{2+} entry by inositol phosphates--a possible mechanism. *FEBS Lett.* **263**, 5-9

Jobling, S. A., and Gehrke, L. (1987). Enhanced translation of chimaeric messenger RNAs containing a plant viral untranslated leader sequence. *Nature* **325**, 622-625

Jurman, M. E., Boland, L. M., Liu, Y., and Yellen, G. (1994) *BioTechniques* **17**, 876-881

Kiselyov, K., Xu, X., Mozhayeva, G., Kuo, T., Pessah, I., Mignery, G., Zhu, X., Birnbaumer, L., Muallem, S. (1998). Functional interaction between $InsP_3$ receptors and store-operated Htrp3 channels. *Nature.* **396**, 478-482

Kozak, M. (1986). Point mutations define a sequence flanking the AUG initiator codon that modulates translation by eukaryotic ribosomes. *Cell* **44**, 283-292

Kuno, M., and Gardner, P. (1987). Ion channels activated by inositol 1,4,5-trisphosphate in plasma membrane of human T-lymphocytes. *Nature* **326**, 301-304

Kyte, J., and Doolittle, R. F. (1982). A simple method for displaying the hydropathic character of a protein. *J. Mol. Biol.* **157**, 105-132

Lacampagne, A., Gannier, F., Argibay, J., Garnier, D., and Le Guennec, J. Y. (1994). The stretch-activated ion channel blocker gadolinium also blocks L-type calcium channels in isolated ventricular myocytes of the guinea-pig. *Biochim. Biophys. Acta* **1191**, 205-208

Luckhoff, A., and Clapham, D. E. (1992). Inositol 1,3,4,5-tetrakisphosphate activates an endothelial Ca^{2+}-permeable channel. *Nature* **355**, 356-358

Lupas, A., Van Dyke, M., and Stock, J. (1991) *Science* **252**, 1162-1164

Montell, C., and Rubin, G. M. (1989). Molecular characterization of the Drosophila trp locus: a putative integral membrane protein required for phototransduction. *Neuron* **2**, 1313-1323

Mori, Y., Friedrich, T., Kim, M.-S., Mikami, A., Nakai, J., Ruth, P., Bosse, E., Hofmann, F., Flockerzi, V., Furuichi, T., Mikoshiba, K., Imoto, K., Tanabe, T., and Numa, S. (1991). Primary structure and functional expression from complementary DNA of a brain calcium channel. *Nature* **350**, 398-402

Mori, Y., Takada, N., Okada, T., Wakamori, M., Imoto, K., Wanifuchi, H., Oka, H., Oba, A., Ikenaka, K., and Kurosaki, T. (1998). Differential distribution of TRP Ca^{2+} channel isoforms in mouse brain. *NeuroReport* **9**, 507-515

Mozhayeva, G. N., Naumov, A. P., and Kuryshev, Y. A. (1991). Variety of Ca^{2+}-permeable channels in human carcinoma A431 cells. *J. Membrane Biol.* **124**, 113-126

Nakagawa, T., Shirasaki, T., Wakamori, M., Fukuda, A., and Akaike, N. (1990). Excitatory amino acid response in isolated nucleus tractus solitarii neurons of the rat. *Neurosci. Res.* **8**, 114-123

Nakanishi, S., Kakita, S., Takahashi, I., Kawahara, K., Tsukuda, E., Sano, T., Yamada, K., Yoshida, M., Kase, H., Matsuda, Y., et al. (1992). Wortmannin, a microbial product inhibitor of myosin light chain kinase. *J Biol Chem.* **267**, 2157-2163

Niemeyer, B. A., Suzuki, E., Scott, K., Jalink, K., and Zuker, C. S. (1996). The Drosophila light-activated conductance is composed of the two channels TRP and TRPL. *Cell* **85**, 651-659

Obukhov, A. G., Harteneck, C., Zobel, A., Harhammer, R., Kalkbrenner, F., Leopoldt, D., Lückhoff, A., Nürnberg, B., and Schultz, G. (1996). Direct activation of trpl cation channels by G alpha11 subunits. *EMBO J.* **15**, 5833-5838

Partiseti, M., Le Deist, F., Hivroz, C., Fischer, A., Korn, H., and Choquet D. (1994). The calcium current activated by T cell receptor and store depletion in human lymphocytes is absent in a primary immunodeficiency. *J. Biol. Chem.* **269**, 32327-32335

Parekh, A. B., Terlau, H., and Stühmer, W. (1993). Depletion of InsP3 stores activates a Ca^{2+} and K^+ current by means of a phosphatase and a diffusible messenger. *Nature* **364**, 814-818

Parekh, A. B., Fleig, A., and Penner, R. (1997). The store-operated calcium current I(CRAC): nonlinear activation by InsP3 and dissociation from calcium release. *Cell* **89**, 973-980

Peretz, A., Abitbol, I., Sobko, A., Wu, C. F., Attali, B. (1998). A Ca2+/calmodulin-dependent protein kinase modulates Drosophila photoreceptor K+ currents: a role in shaping the photoreceptor potential. *J Neurosci.* **18**, 9153-9162

Petersen, C. C. H., and Berridge, M. J. (1994). The regulation of capacitative calcium entry by calcium and protein kinase C in Xenopus oocytes. *J. Biol. Chem.* **269**, 32246-32253

Petersen, C. C. H., Berridge, M. J., Borgese, M. F., and Bennett, D. L. (1995). Putative capacitative calcium entry channels: expression of Drosophila trp and evidence for the existence of vertebrate homologues. *Biochem. J.* **311**, 41-44

Philipp, S., Cavalié, A., Freichel, M., Wissenbach, U., Zimmer, S., Trost, C., Marquart, A., Murakami, M., and Flockerzi, V. (1996). A mammalian capacitative calcium entry channel homologous to Drosophila TRP and TRPL. *EMBO J.* **15**, 6166-6171

Phillips, A. M., Bull, A., and Kelly, L. E. (1992). Identification of a Drosophila gene encoding a calmodulin-binding protein with homology to the trp phototransduction gene. *Neuron* **8**, 631-642

Preuß, K.-D., Nöller, J. K., Krause, E., Göbel, A., and Schulz, I. (1997). Expression and characterization of a trpl homolog from rat. *Biochem. Biophys. Res. Commun.* **240**, 167-172

Putney, J. W. (1990). Capacitative calcium entry revisited. *Cell Calcium* **11**, 611-624

Putney, J. W., and Bird, G. St. J. (1993). The signal for capacitative calcium entry. *Cell* **75**, 199-201

Randriamampita, C., and Tsien, R. Y. (1993). Emptying of intracellular Ca^{2+} stores releases a novel small messenger that stimulates Ca2+ influx. *Nature* **364**, 809-814

Ranganathan, R., Malicki, D. M., and Zuker, C. S. (1995). Signal transduction in Drosophila photoreceptors. *Annu. Rev. Neurosci.* **18**, 283-317

Restrepo, D., Miyamoto, T., Bryant, B. P., and Teeter, J. H. (1990). Odor stimuli trigger influx of calcium into olfactory neurons of the channel catfish. *Science* **249**, 1166-1168

Saitou, N., and Nei, M. (1987). The neighbor-joining method: a new method for reconstructing phylogenetic trees. *Mol. Biol. Evol.* **4**, 406-425

Sakura, H., and Ashcroft, F. M. (1997). Identification of four trp1 gene variants murine pancreatic beta-cells. *Diabetologia* **40**, 528-532

Serafini, A. T., Lewis, R. S., Clipstone, N. A., Bram, R. J., Fanger, C., Fiering, S., Herzenberg, L. A., and Crabtree, G. R. (1995). Isolation of mutant T lymphocytes with defects in capacitative calcium entry. *Immunity* **3**, 239-250

Sinkins, W. G., Vaca, L., Hu, Y., Kunze, D. L., and Schilling, W. P. (1996). The COOH-terminal domain of Drosophila TRP channels confers thapsigargin sensitivity. *J. Biol. Chem.* **271**, 2955-2960

Sulston, J., Du, Z., Thomas, K., Wilson, R., Hillier, L., Staden, R., Halloran, N., Green, P., Thierry-Mieg, J., Qiu, L., Dear, S., Coulson, A., Craxton, M., Durbin, R., Berks, M., Metzstein, M., Hawkins, T., Ainscough, R., and Waterston, R. (1992). The C. elegans genome sequencing project: a beginning. *Nature* **356**, 37-41

Thompson, J. D., Higgins, D. G., and Gibson, T. J. (1994). CLUSTAL W: improving the sensitivity of progressive multiple sequence alignment through sequence weighting, position-specific gap penalties and weight matrix choice. *Nucleic Acids Res.* **22**, 4673-4680

Tsien, R. W., and Tsien, R. Y. (1990). Calcium channels, stores, and oscillations. *Annu. Rev. Cell Biol.* **6**, 715-760

Ueda, S., and Okada, Y. (1989). Acid secretagogues induce Ca^{2+} mobilization coupled to K^+ conductance activation in rat parietal cells in tissue culture. *Biochim. Biophys. Acta* **1012**, 254-260

Vaca, L., Sinkins, W. G., Hu, Y., Kunze, D. L., and Schilling, W. P. (1994). Activation of recombinant trp by thapsigargin in Sf9 insect cells. *Am. J. Physiol.* **267**, C1501-C1505

Waldron, R. T., Short, A. D., and Gill, D. L. (1997). Store-operated Ca^{2+} entry and coupling to Ca^{2+} pool depletion in thapsigargin-resistant cells. *J. Biol. Chem.* **272**, 6440-6447

Watanabe, H., Takahashi, R., Zhang, X.X., Kakizawa, H., Hayashi, H., and Ohno, R. (1996). Inhibition of agonist-induced Ca2+ entry in endothelial cells by myosin light-chain kinase inhibitor. *Biochem Biophys Res Commun.* **225**, 777-784.

Wes, P. D., Chevesich, J., Jeromin, A., Rosenberg, C., Stetten, G., and Montell, C. (1995). TRPC1, a human homolog of a Drosophila store-operated channel. *Proc. Natl. Acad. Sci. USA* **92**, 9652-9656

Xu, X.-Z. S., Li, H.-S., Guggino, W. B., and Montell, C. (1997). Coassembly of TRP and TRPL produces a distinct store-operated conductance. *Cell* **89**, 1155-1164

Zhu, X., Chu, P. B., Peyton, M., and Birnbaumer, L. (1995). Molecular cloning of a widely expressed human homologue for the Drosophila trp gene. *FEBS Lett.* **373**, 193-198

Zhu, X., Jiang, M., Birnbaumer, L. (1998). Receptor-activated Ca^{2+} influx via human Trp3 stably expressed in human embryonic kidney (HEK)293 cells. Evidence for a non-capacitative Ca2+ entry. *J. Biol. Chem.* **273**, 133-142

Zhu, X., Jiang, M., Peyton, M., Boulay, G., Hurst, R., Stefani, E., and Birnbaumer, L. (1996). trp, a novel mammalian gene family essential for agonist-activated capacitative Ca^{2+} entry. *Cell* **85**, 661-671

Zitt, C., Zobel, A., Obukhov, A. G., Harteneck, C., Kalkbrenner, F., Lückhoff, A., and Schultz, G. (1996) *Neuron* **16**, 1189-1196

Zitt, C., Obukhov, A. G., Strübing, C., Zobel, A., Kalkbrenner, F., Lückhoff, A., and Schultz, G. (1997). Expression of TRPC3 in Chinese hamster ovary cells results in calcium-activated cation currents not related to store depletion. *J. Cell Biol.* **138**, 1333-1341

Figure 1A

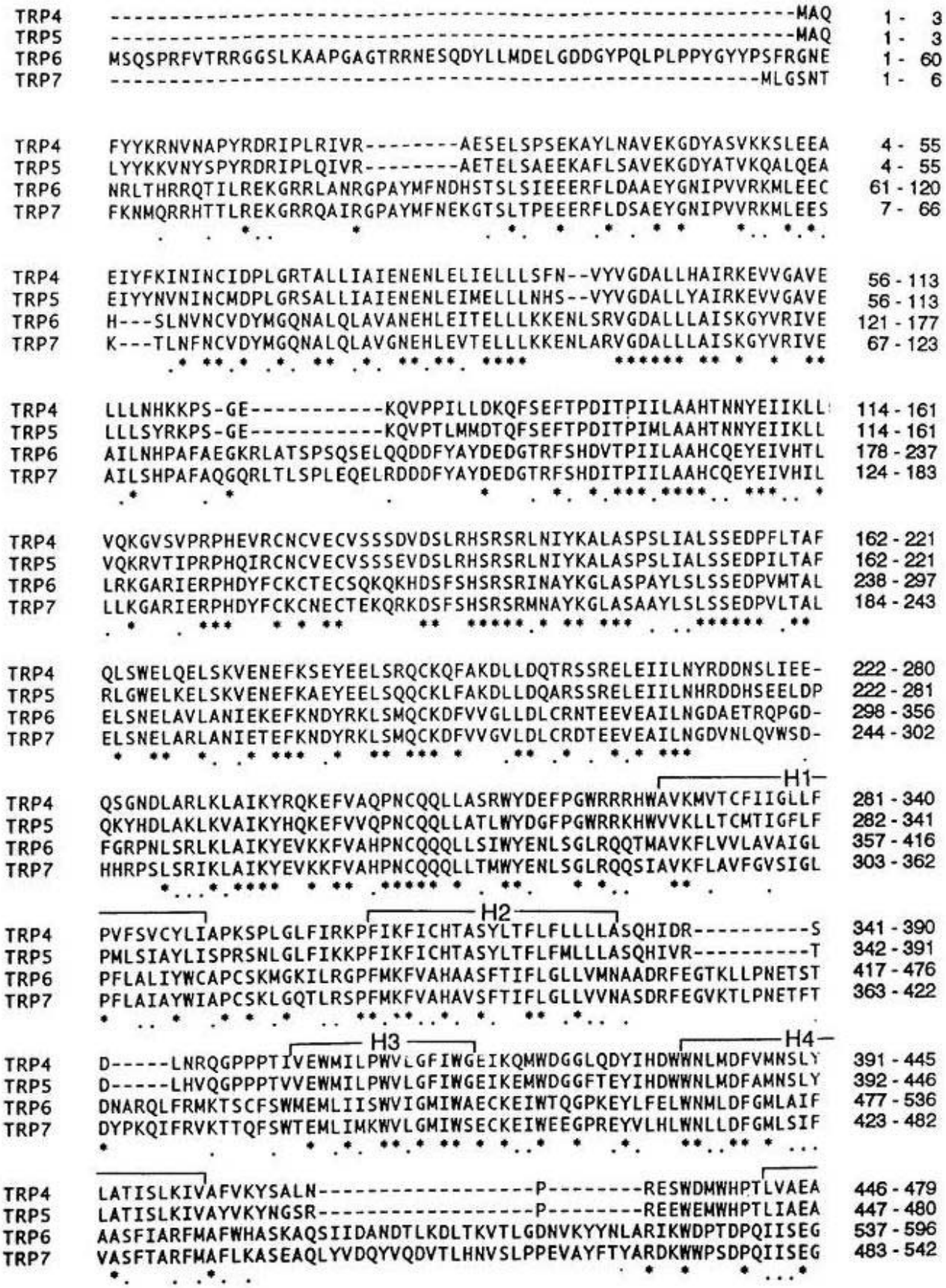
TRP4 ----------MAQ 1 - 3
TRP5 ----------MAQ 1 - 3
TRP6 MSQSPRFVTRRGGSLKAAPGAGTRRNESQDYLLMDELGDDGYPQLPLPPYGYYPSFRGNE 1 - 60
TRP7 ----------MLGSNT 1 - 6
TRP4 FYYKRNVNAPYRDRIPLRIVR--------AESELSPSEKAYLNAVEKGDYASVKKSLEEA 4 - 55
TRP5 LYYKKVNYSPYRDRIPLQIVR--------AETELSAEEKAFLSAVEKGDYATVKQALQEA 4 - 55
TRP6 NRLTHRRQTILREKGRRLANRGPAYMFNDHSTSLSIEEERFLDAAEYGNIPVVRKMLEEC 61 - 120
TRP7 FKNMQRRHTTLREKGRRQAIRGPAYMFNEKGTSLTPEEERFLDSAEYGNIPVVRKMLEES 7 - 66
TRP4 EIYFKININCIDPLGRTALLIAIENENLELIELLLSFN--VYVGDALLHAIRKEVVGAVE 56 - 113
TRP5 EIYYNVNINCMDPLGRSALLIAIENENLEIMELLLNHS--VYVGDALLYAIRKEVVGAVE 56 - 113
TRP6 H---SLNVNCVDYMGQNALQLAVANEHLEITELLLKKENLSRVGDALLLAISKGYVRIVE 121 - 177
TRP7 K---TLNFNCVDYMGQNALQLAVGNEHLEVTELLLKKENLARVGDALLLAISKGYVRIVE 67 - 123
TRP4 LLLNHKKPS-GE----------KQVPPILLDKQFSEFTPDITPIILAAHTNNYEIIKLL 114 - 161
TRP5 LLLSYRKPS-GE----------KQVPTLMMDTQFSEFTPDITPIMLAAHTNNYEIIKLL 114 - 161
TRP6 AILNHPAFAEGKRLATSPSQSELQQDDFYAYDEDGTRFSHDVTPIILAAHCQEYEIVHTL 178 - 237
TRP7 AILSHPAFAQGQRLTLSPLEQELRDDDFYAYDEDGTRFSHDITPIILAAHCQEYEIVHIL 124 - 183
TRP4 VQKGVSVPRPHEVRCNCVECVSSSDVDSLRHSRSRLNIYKALASPSLIALSSEDPFLTAF 162 - 221
TRP5 VQKRVTIPRPHQIRCNCVECVSSSEVDSLRHSRSRLNIYKALASPSLIALSSEDPILTAF 162 - 221
TRP6 LRKGARIERPHDYFCKCTECSQKQKHDSFSHSRSRINAYKGLASPAYLSLSSEDPVMTAL 238 - 297
TRP7 LLKGARIERPHDYFCKCNECTEKQRKDSFSHSRSRMNAYKGLASAAYLSLSSEDPVLTAL 184 - 243
TRP4 QLSWELQELSKVENEFKSEYEELSRQCKQFAKDLLDQTRSSRELEIILNYRDDNSLIEE- 222 - 280
TRP5 RLGWELKELSKVENEFKAEYEELSQQCKLFAKDLLDQARSSRELEIILNHRDDHSEELDP 222 - 281
TRP6 ELSNELAVLANIEKEFKNDYRKLSMQCKDFVVGLLDLCRNTEEVEAILNGDAETRQPGD- 298 - 356
TRP7 ELSNELARLANIETEFKNDYRKLSMQCKDFVVGVLDLCRDTEEVEAILNGDVNLQVWSD- 244 - 302
H1
TRP4 QSGNDLARLKLAIKYRQKEFVAQPNCQQLLASRWYDEFPGWRRRHWAVKMVTCFIIGLLF 281 - 340
TRP5 QKYHDLAKLKVAIKYHQKEFVVQPNCQQLLATLWYDGFPGWRRKHWVVKLLTCMTIGFLF 282 - 341
TRP6 FGRPNLSRLKLAIKYEVKKFVAHPNCQQQLLSIWYENLSGLRQQTMAVKFLVVLAVAIGL 357 - 416
TRP7 HHRPSLSRIKLAIKYEVKKFVAHPNCQQQLLTMWYENLSGLRQQSIAVKFLAVFGVSIGL 303 - 362
H2
TRP4 PVFSVCYLIAPKSPLGLFIRKPFIKFICHTASYLTFLFLLLLASQHIDR----------S 341 - 390
TRP5 PMLSIAYLISPRSNLGLFIKKPFIKFICHTASYLTFLFMLLLASQHIVR----------T 342 - 391
TRP6 PFLALIYWCAPCSKMGKILRGPFMKFVAHAASFTIFLGLLVMNAADRFEGTKLLPNETST 417 - 476
TRP7 PFLAIAYWIAPCSKLGQTLRSPFMKFVAHAVSFTIFLGLLVVNASDRFEGVKTLPNETFT 363 - 422
H3
H4
TRP4 D-----LNRQGPPPTIVEWMILPWVLGFIWGEIKQMWDGGLQDYIHDWWNLMDFVMNSLY 391 - 445
TRP5 D-----LHVQGPPPTVVEWMILPWVLGFIWGEIKEMWDGGFTEYIHDWWNLMDFAMNSLY 392 - 446
TRP6 DNARQLFRMKTSCFSWMEMLIISWVIGMIWAECKEIWTQGPKEYLFELWNMLDFGMLAIF 477 - 536
TRP7 DYPKQIFRVKTTQFSWTEMLIMKWVLGMIWSECKEIWEEGPREYVLHLWNLLDFGMLSIF 423 - 482
TRP4 LATISLKIVAFVKYSALN----------P--------RESWDMWHPTLVAEA 446 - 479
TRP5 LATISLKIVAYVKYNGSR----------P--------REEWEMWHPTLIAEA 447 - 480
TRP6 AASFIARFMAFWHASKAQSIIDANDTLKDLTKVTLGDNVKYYNLARIKWDPTDPQIISEG 537 - 596
TRP7 VASFTARFMAFLKASEAQLYVDQYVQDVTLHNVSLPPEVAYFTYARDKWWPSDPQIISEG 483 - 542

Figure 1A continued

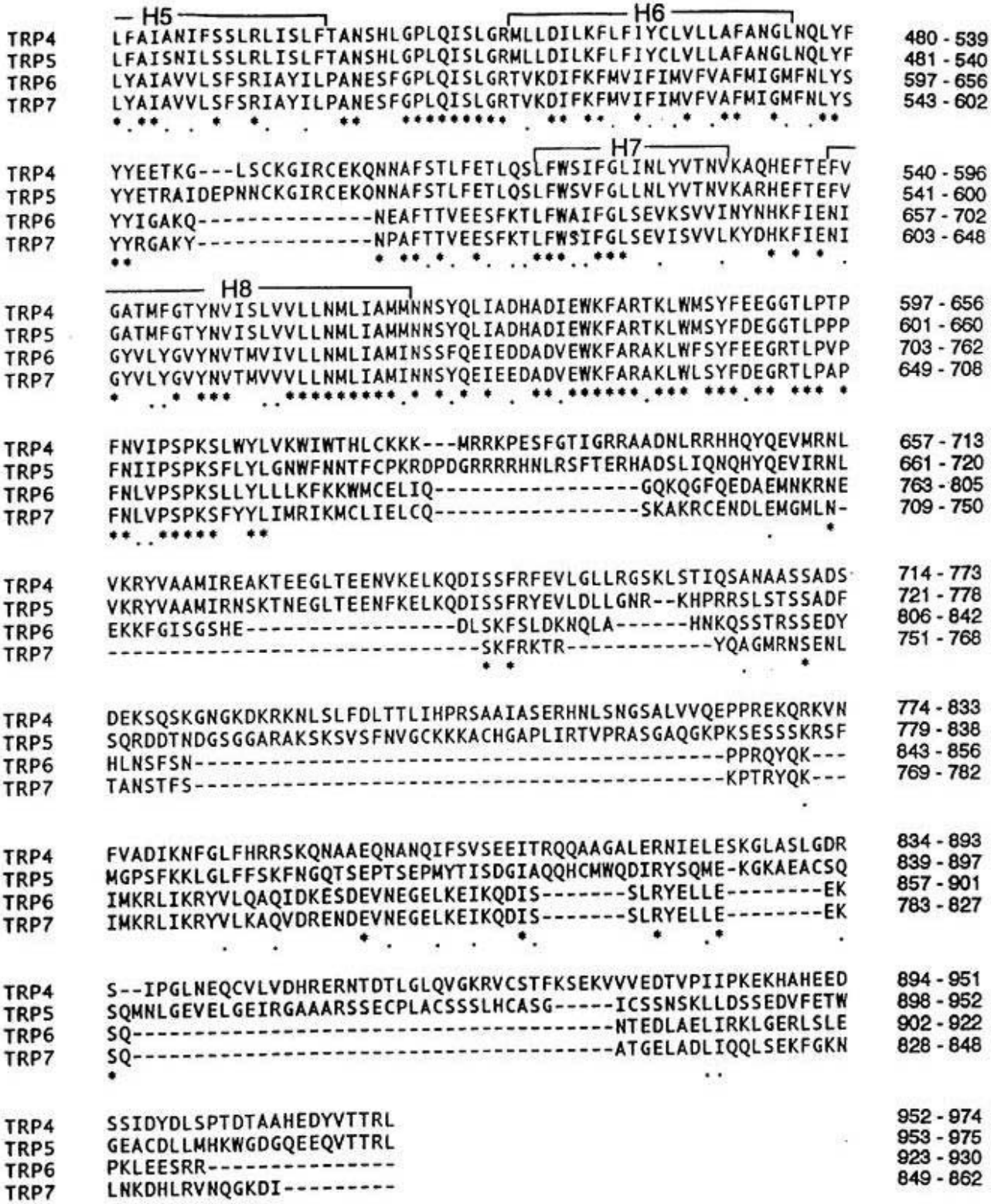

Figure 1 continued

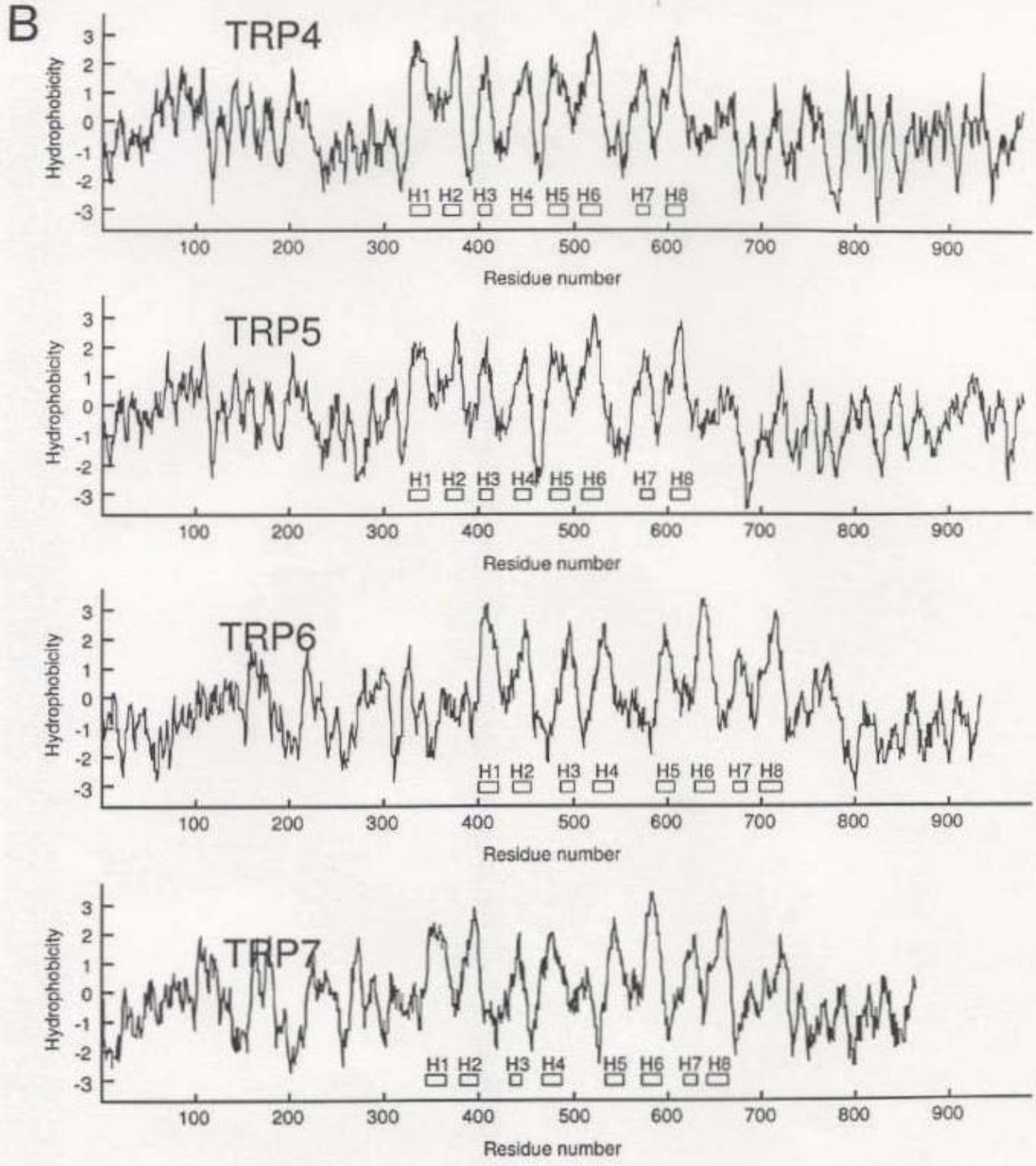

Figure 1 continued

D

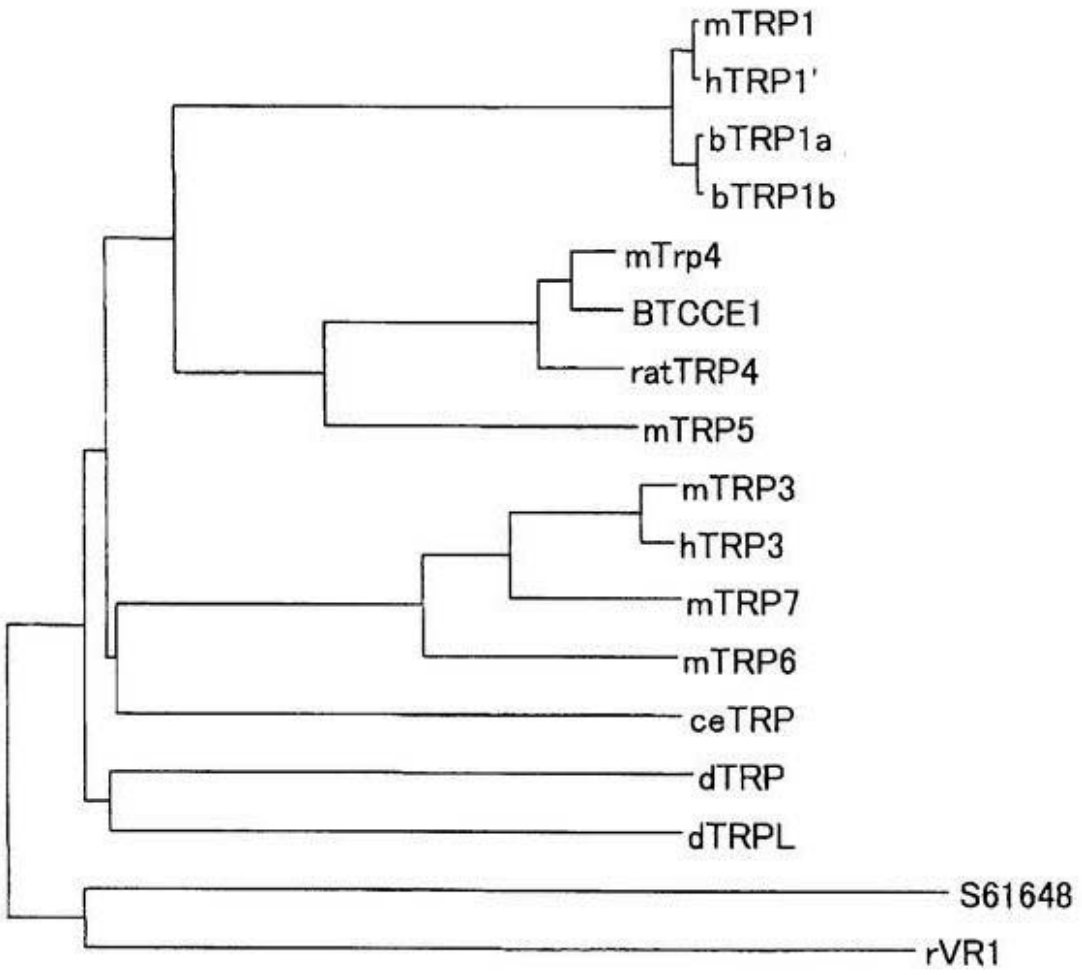

FIG. 1. **Primary structure and hydropathy analysis of TRP4, TRP5, TRP6 and TRP7, and phylogenetic tree of the TRP family.** In *A*, the amino acid sequences (in *single letter code*) of the mouse TRP4, TRP5, TRP6, and TRP7 aligned using the Clustalw program (Thompson et al., 1994) are shown. The hydrophobic regions H1-H8 are shown. Sets of four identical residues at one position are marked with asterisks, and sets of four conservative residues at one position with dots under them. In *B*, the Kyte-Doolittle hydrophobicity profiles of TRP4, TRP5, TRP6, and TRP7 were generated with the window size of 10 amino acids (Kyte and Doolittle, 1982). *C*, Putative transmembrane topology of TRP homologues. In *D*, the phylogenetic tree for the TRP family and the capsaicin receptor (rVR1, Caterina et al., 1997) was generated using the Clustalw program. Additional members of the TRP family are as follows: dTRP (d: *Drosophila*, Montell and Rubin, 1989), dTRPL (Phillips et al., 1992), mTRP1 (m: Mus musculus, Sakura and Aschcroft, 1997), hTRP1(h: Homo sapiens, Wes et al., 1995), bTRP1a and bTRP1b (b: Bos taurus, Chang et al., 1997), mTRP3 (Mori et al., 1998), hTRP3 (Zhu et al., 1996), BTCCE1 (bTRP4, Philipp et al., 1996), ratTRP4 (rat, r: Rattus norvegicus, Funayama et al., 1996), ceTRP (ce: *C. elegans*, Sulston et al., 1992), S61648 (*S. cerevisiae*, accession No.).

Figure 2

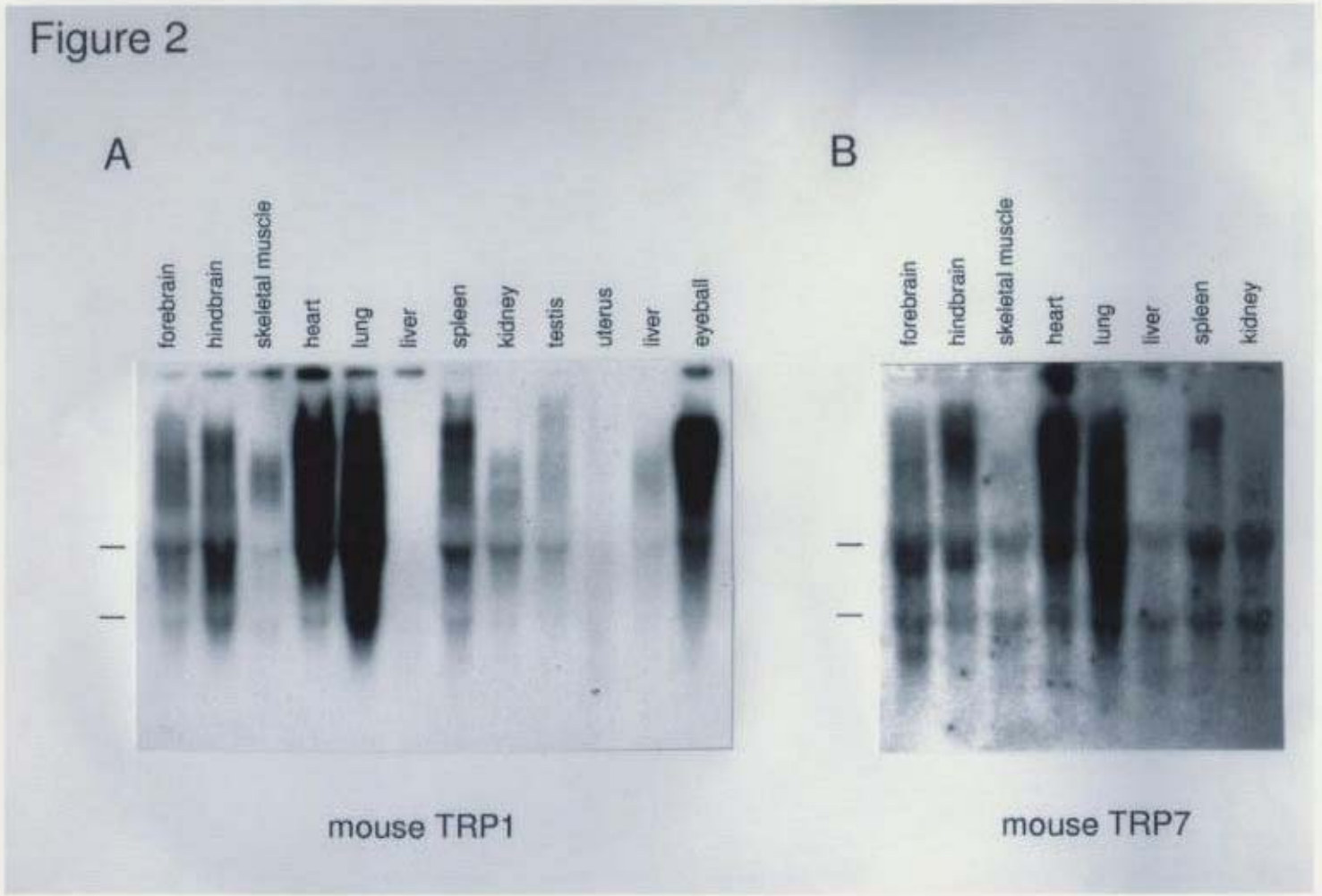
A
forebrain
hindbrain
skeletal muscle
heart
lung
liver
spleen
kidney
testis
uterus
liver
eyeball
mouse TRP1
B
forebrain
hindbrain
skeletal muscle
heart
lung
liver
spleen
kidney
mouse TRP7

Figure 2 continued

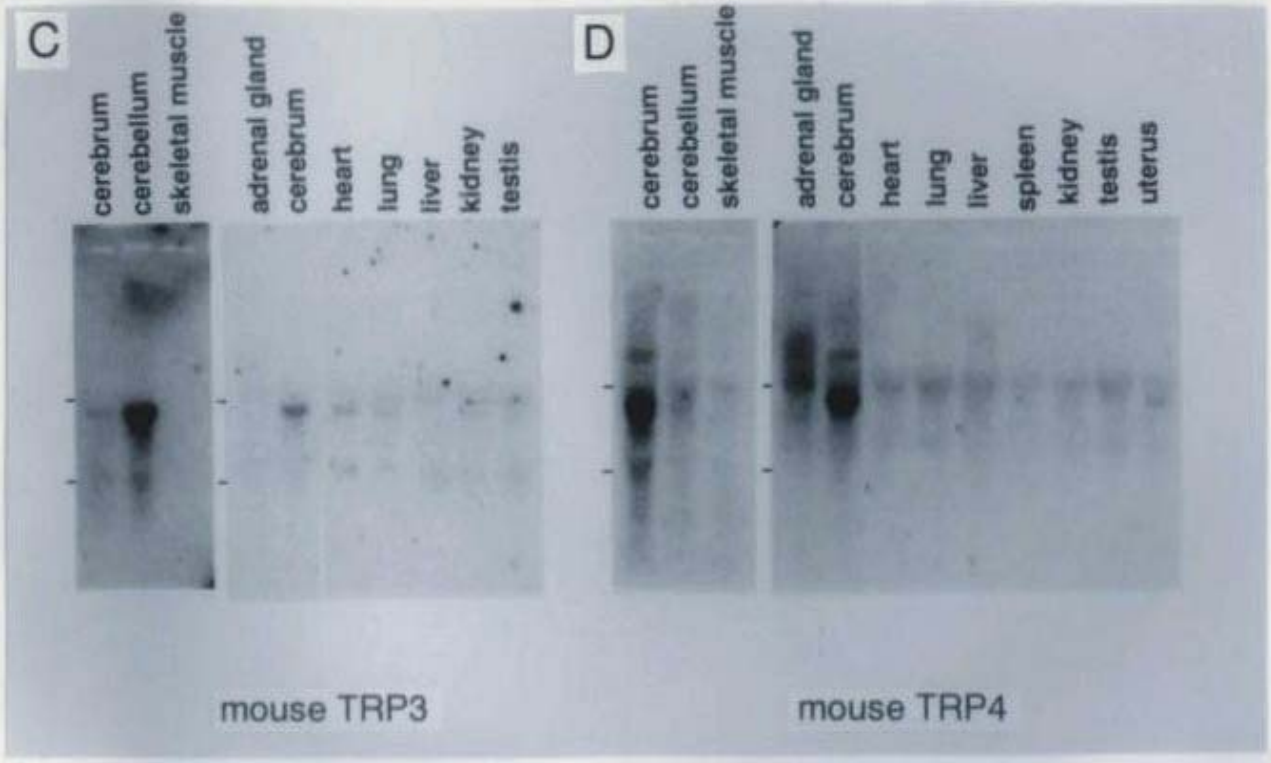

Figure 2 continued

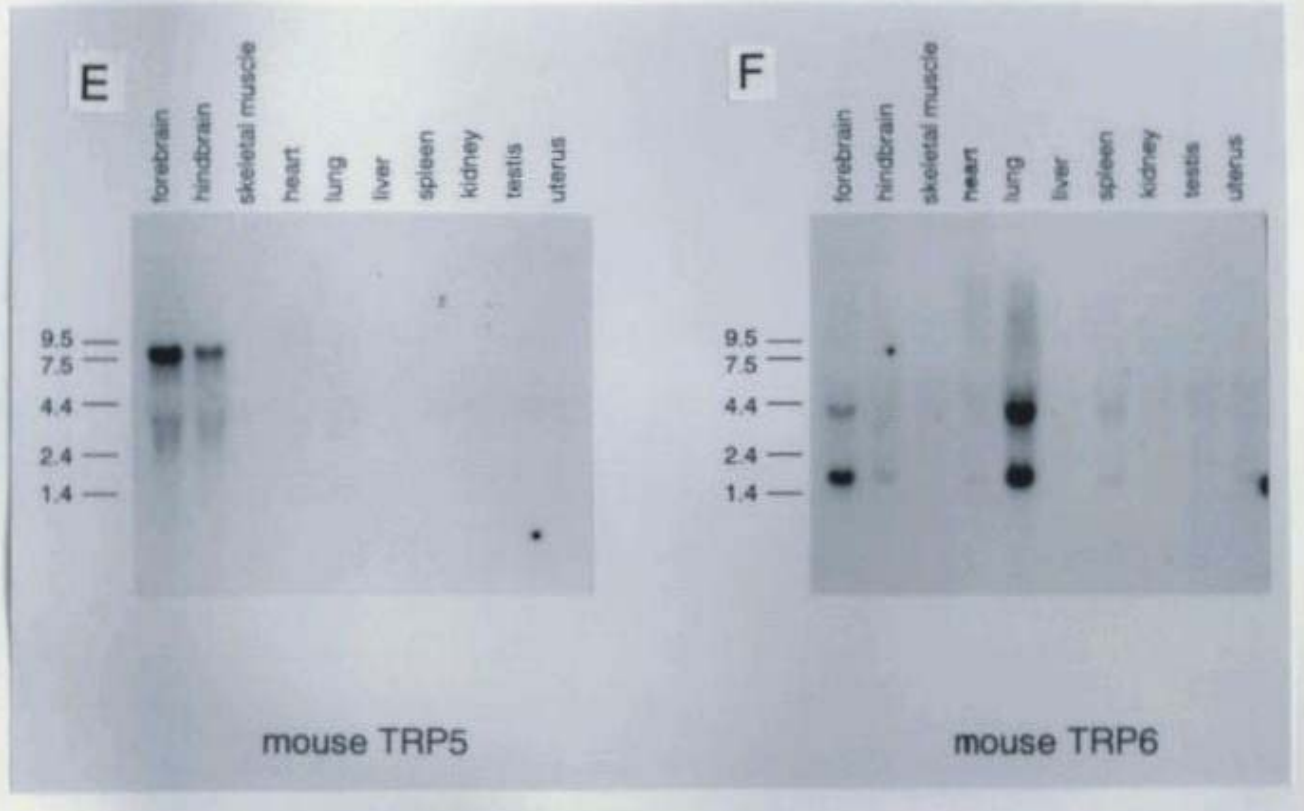

Figure 2 continued

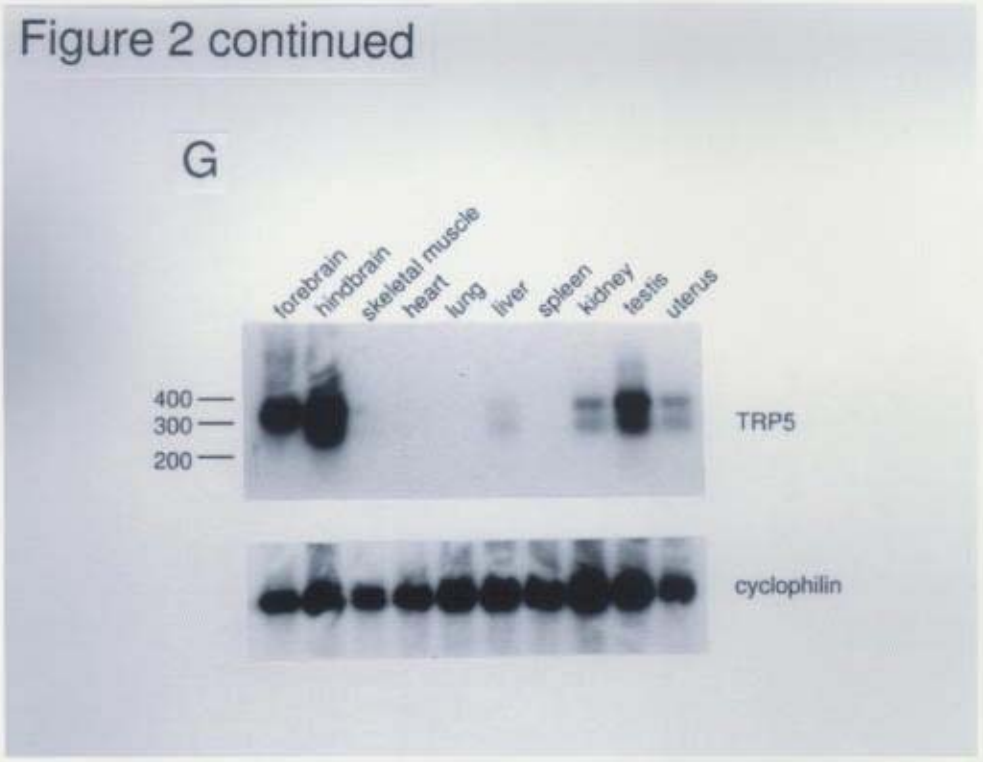

FIG. 2. **Distribution of TRP5 mRNA expression in the mouse tissues.** Autoradiograms of blot hybridization analysis of RNA from different tissues of mice with cDNA probes of TRP1 (*A*), TRP3 (*C*), TRP4 (*D*), TRP5 (*E*), TRP6 (*F*), and TRP7 (*B*). The positions and sizes (in kb) of the RNA markers or the positions of the ribosomal RNAs (18S and 28S) are shown on the left. *G*, autoradiogram of blot hybridization analyses of TRP5 and cyclophilin cDNA fragments amplified by RT-PCR. Probes are 5' end-labeled oligonucleotides internal to the primers used for PCR. The positions and sizes (in base-pair) of DNA markers are shown on the *left*.

Figure 3

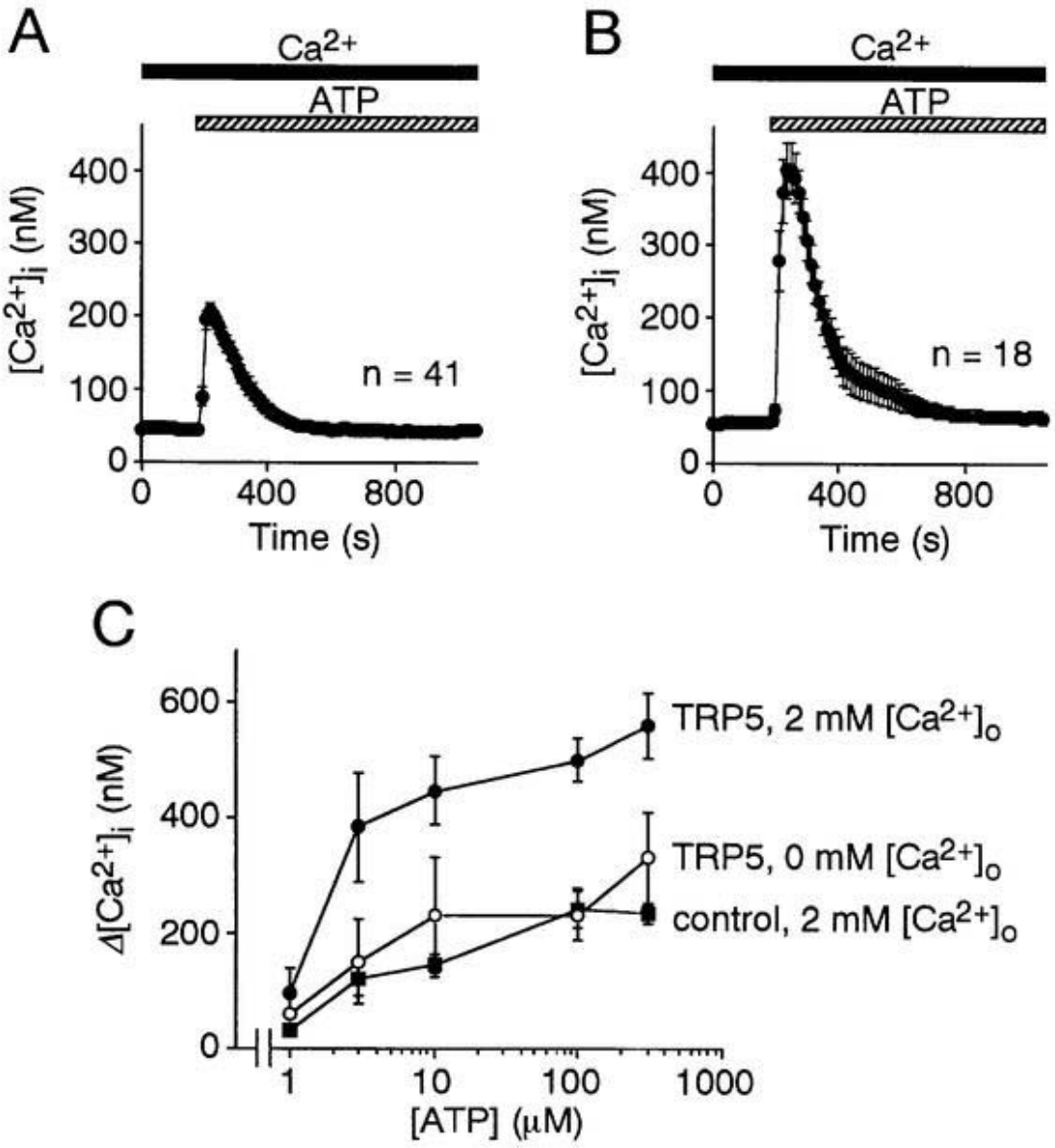
A
Ca2+
ATP
[Ca2+]i (nM)
400
300
200
100
0
n = 41
0
400
800
Time (s)
B
Ca2+
ATP
[Ca2+]i (nM)
400
300
200
100
0
n = 18
0
400
800
Time (s)
C
Δ[Ca2+]i (nM)
600
400
200
0
1
10
100
1000
[ATP] (μM)
TRP5, 2 mM [Ca2+]o
TRP5, 0 mM [Ca2+]o
control, 2 mM [Ca2+]o

FIG. 3. **ATP-induced $[Ca^{2+}]_i$ transients in control and TRP5-transfected HEK cells in the presence of extracellular Ca^{2+}.** Cytosolic Ca^{2+} was measured in fura-2-loaded control HEK293 cells (*A*) or HEK293 cells transfected with TRP5 plus CD8 (*B*). The cells were treated with 100 μM ATP in the presence of 2 mM extracellular Ca^{2+}. The duration of exposure to Ca^{2+}-containing HBS and 100 μM ATP is indicated by the *filled* and *hatched bars*, respectively, above the graphs. *C*, dose-response relationships for maximum ATP-induced $[Ca^{2+}]_i$ rises ($\Delta[Ca^{2+}]_i$) in individual control HEK293 cells (*filled box*) or HEK293 cells transfected with TRP5 plus CD8 cDNAs (*filled circle*) in the presence of 2 mM extracellular Ca^{2+}, and in TRP5-transfected cells in the absence of extracellular Ca^{2+} (*open circle*). Data points are the means ± SEM $[Ca^{2+}]_i$ or the means ± SEM $\Delta[Ca^{2+}]_i$ in 30-41 control HEK cells or 14-20 TRP5-transfected cells.

Figure 4

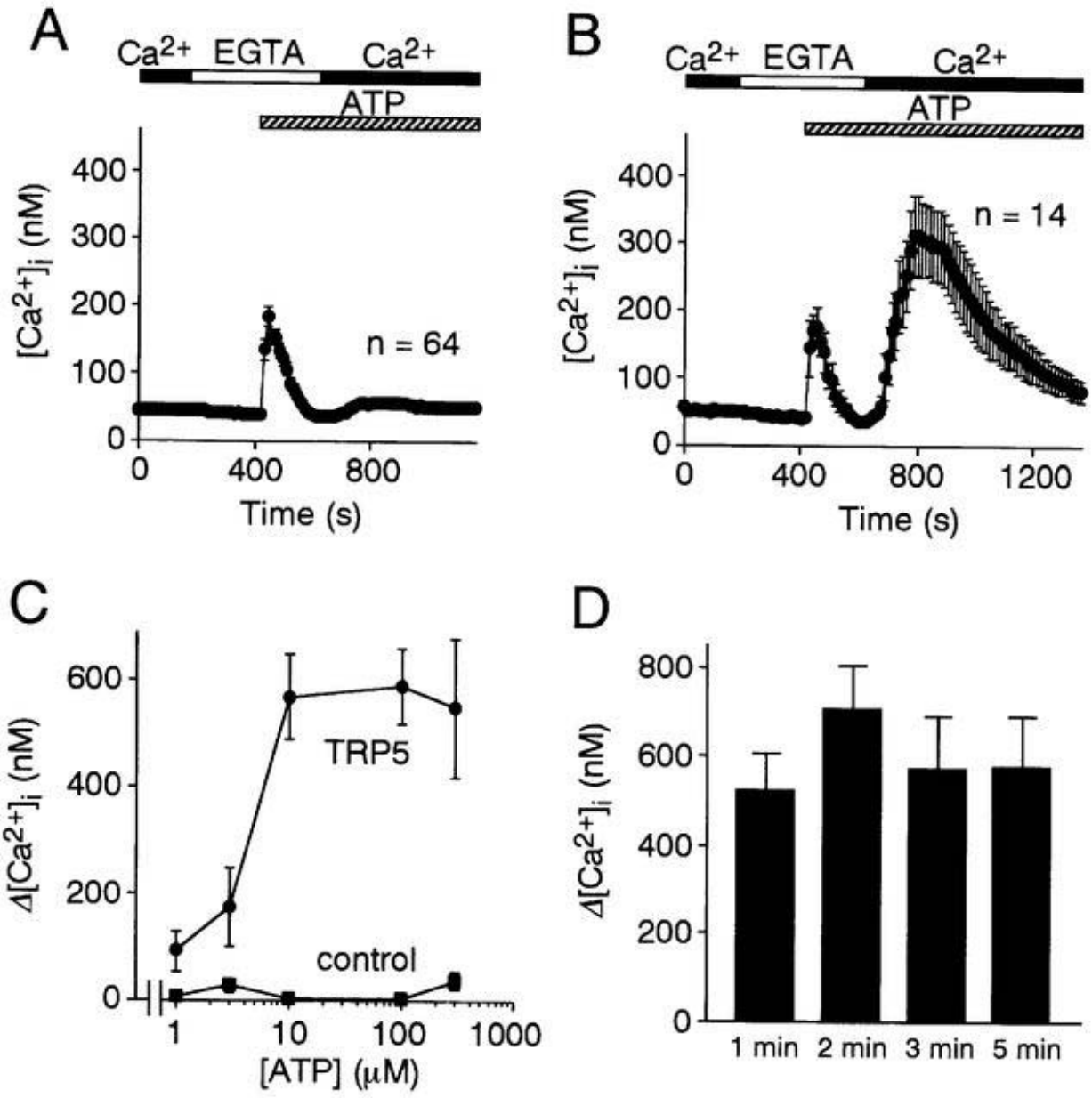
A
Ca2+ EGTA Ca2+
ATP
[Ca2+]i (nM)
400
300
200
100
0
n = 64
0
400
800
Time (s)
B
Ca2+ EGTA Ca2+
ATP
[Ca2+]i (nM)
400
300
200
100
0
n = 14
0
400
800
1200
Time (s)
C
Δ[Ca2+]i (nM)
600
400
200
0
TRP5
control
1
10
100
1000
[ATP] (μM)
D
Δ[Ca2+]i (nM)
800
600
400
200
0
1 min
2 min
3 min
5 min

FIG. 4. **Separation of ATP-induced $[Ca^{2+}]_i$ transients due to Ca^{2+} release from internal stores and Ca^{2+} influx in TRP5-transfected HEK cells.** Cytosolic Ca^{2+} was measured in fura-2-loaded control HEK293 cells (*A*) or HEK293 cells transfected with TRP5 plus CD8 (*B*). In *A* and *B*, the perfusion solution was first changed to Ca^{2+}-free HBS containing 0.5 mM EGTA, and 100 μM ATP was applied to the cells in the absence of extracellular Ca^{2+}. Three min after the application of ATP, 2 mM Ca^{2+} was further added to the extracellular solution. The duration of exposure to Ca^{2+}-containing HBS, Ca^{2+}-free HBS, and 100 μM ATP is indicated by the *filled*, *open*, and *hatched bars*, respectively, above the graphs. *C*, ATP concentration dependence of maximum $[Ca^{2+}]_i$ rises ($\Delta[Ca^{2+}]_i$) induced by the addition of 2 mM extracellular Ca^{2+} 3 min after the addition of ATP in individual control HEK293 cells (*filled box*) and HEK293 cells transfected with TRP5 plus CD8 (*filled circle*). *D*, $\Delta[Ca^{2+}]_i$ in TRP5-transfected cells are shown for various time intervals between the initiation of ATP (100 μM) application and the addition of 2 mM extracellular Ca^{2+}. Small $\Delta[Ca^{2+}]_i$ for 1 min resulted from $[Ca^{2+}]_i$ which was not yet reduced to the basal level before the addition of extracellular Ca^{2+}. Data points and columns are the means ± SEM $[Ca^{2+}]_i$ or the means ± SEM $\Delta[Ca^{2+}]_i$ in 29-64 control HEK cells or 14-16 TRP5-transfected cells.

Figure 5

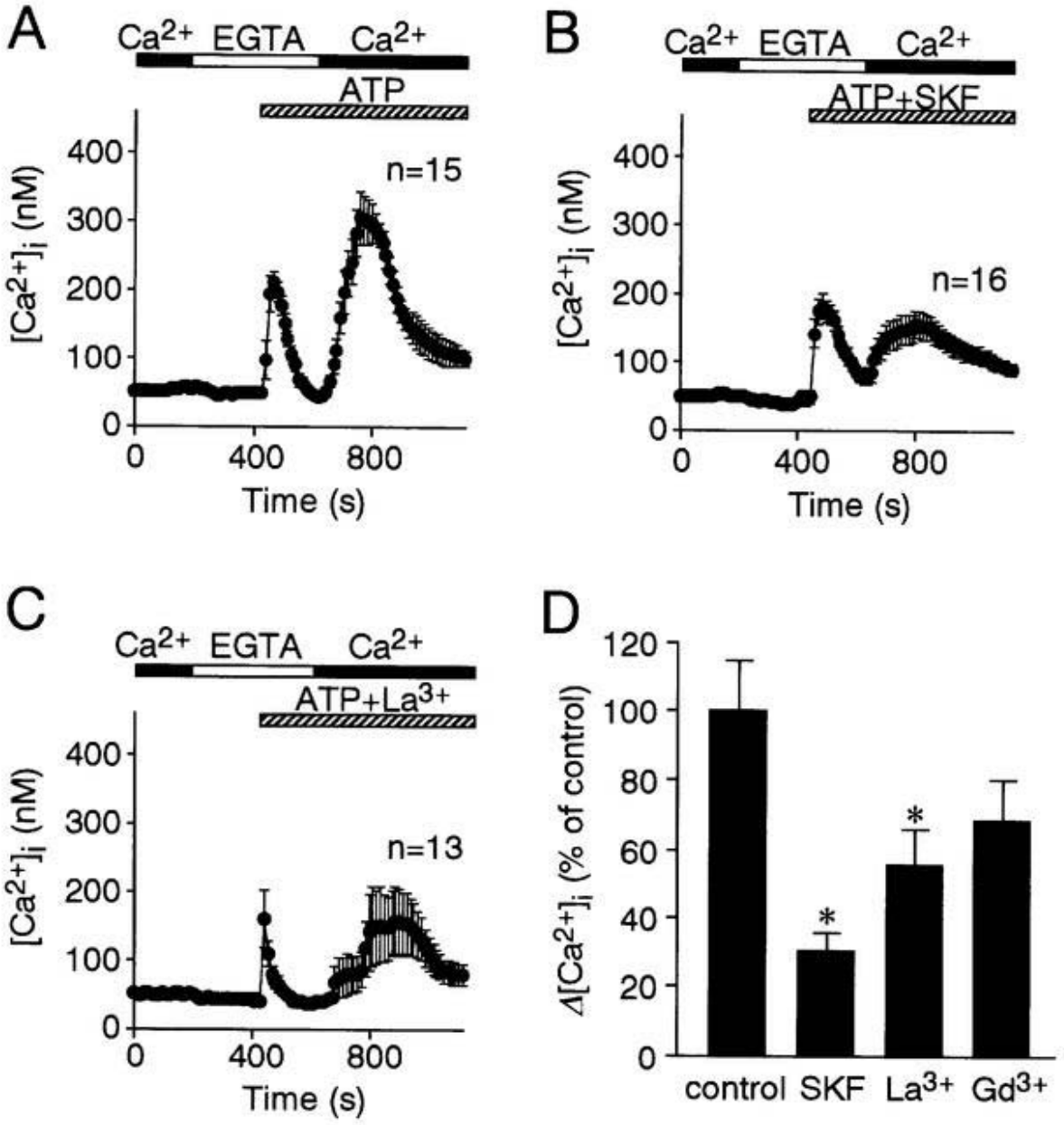
A
Ca2+ EGTA Ca2+
ATP
n=15
[Ca2+]i (nM)
Time (s)
B
Ca2+ EGTA Ca2+
ATP+SKF
n=16
[Ca2+]i (nM)
Time (s)
C
Ca2+ EGTA Ca2+
ATP+La3+
n=13
[Ca2+]i (nM)
Time (s)
D
Δ[Ca2+]i (% of control)
control SKF La3+ Gd3+

FIG. 5. **Pharmacological properties of ATP-induced Ca^{2+} influx in TRP5-transfected HEK cells.** Cytosolic Ca^{2+} was measured in fura-2-loaded TRP5-transfected cells. The perfusion solution was changed to Ca^{2+}-free HBS, and 100 μM ATP alone (*A* and *D*), with 25 μM SK&F96365 (*B* and *D*), with 100 μM $LaCl_3$ (*C* and *D*), or with 100 μM $GdCl_3$ (*D*) was applied to the cells in the absence of extracellular Ca^{2+}, which was followed by the addition of 2 mM extracellular Ca^{2+}. The duration of exposure to Ca^{2+}-containing HBS, Ca^{2+}-free HBS, and 100 μM ATP alone or plus one of the drugs is indicated by the *filled*, *open*, and *hatched bars*, respectively, above the graphs. *D*, Effects of 25 μM SK&F96365, 100 μM $LaCl_3$, and 100 μM $GdCl_3$ on the amplitude of maximum $[Ca^{2+}]_i$ rises ($\Delta[Ca^{2+}]_i$) induced by the addition of 2 mM extracellular Ca^{2+} 3 min after the addition of ATP in individual TRP5-transfected cells. For the experiments using lanthanides and their control experiments, KH_2PO_4 was omitted from HBS. The data shown in *A* are from the experiments using the phosphate-containing solution. SEM from the experiments using the phosphate-free external solutions is shown for control $\Delta[Ca^{2+}]_i$ shown in *D*. Data points and columns are the means ± SEM $[Ca^{2+}]_i$ or the means ± SEM $\Delta[Ca^{2+}]_i$ in 13-21 TRP5-transfected cells. Bonferroni's *t* test following analysis of variance was employed to determine the statistical significance of differences. *, $p < 0.05$, compared with the control.

Figure 6

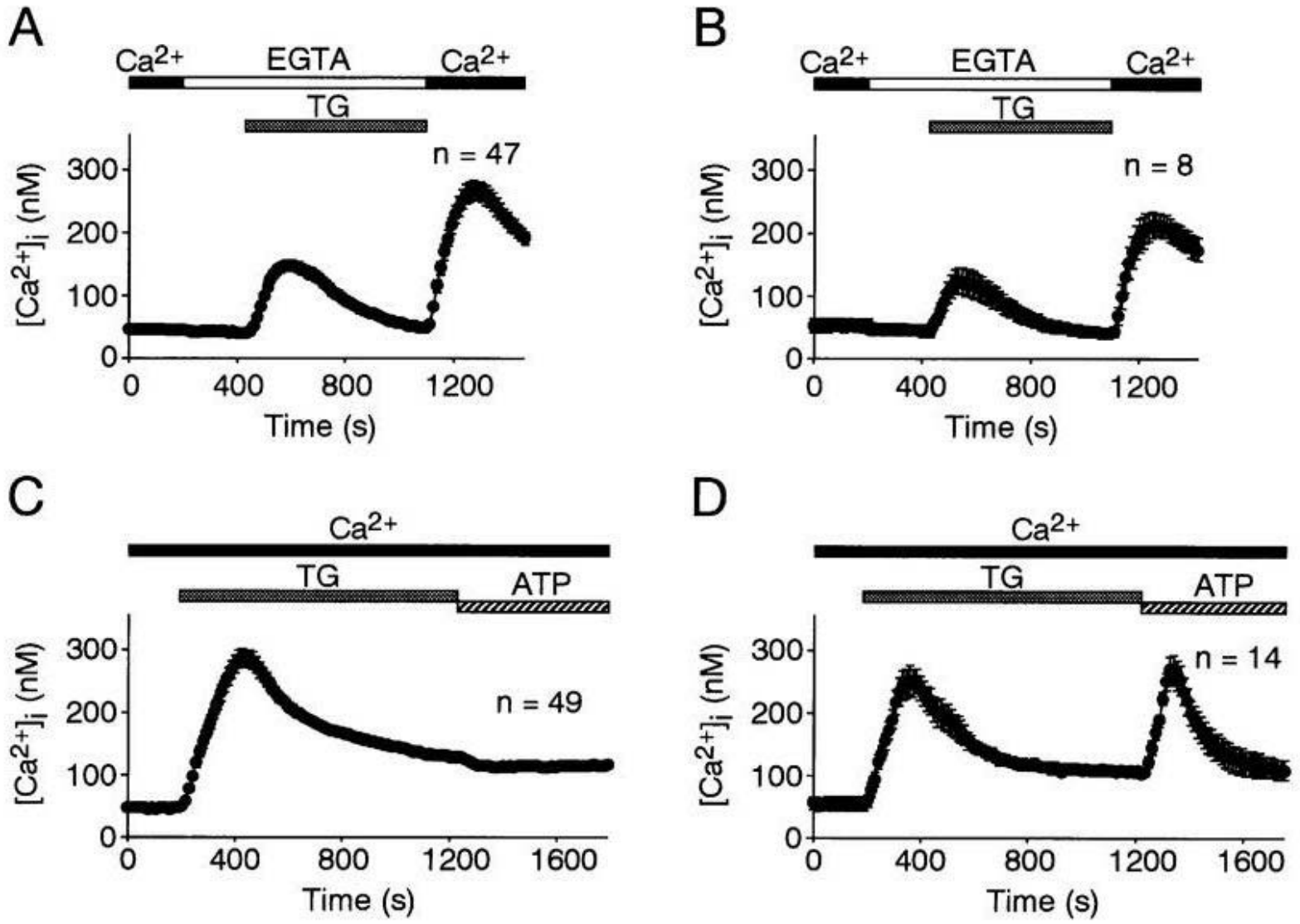
A
Ca2+
EGTA
Ca2+
TG
n = 47
[Ca2+]i (nM)
300
200
100
0
0
400
800
1200
Time (s)
B
Ca2+
EGTA
Ca2+
TG
n = 8
[Ca2+]i (nM)
300
200
100
0
0
400
800
1200
Time (s)
C
Ca2+
TG
ATP
n = 49
[Ca2+]i (nM)
300
200
100
0
0
400
800
1200
1600
Time (s)
D
Ca2+
TG
ATP
n = 14
[Ca2+]i (nM)
300
200
100
0
0
400
800
1200
1600
Time (s)

FIG. 6. **Thapsigargin-induced $[Ca^{2+}]_i$ transients and ATP-induced $[Ca^{2+}]_i$ changes after store depletion in control and TRP5-transfected HEK cells.** Cytosolic Ca^{2+} was measured in fura-2-loaded control HEK293 cells (*A* and *C*) or HEK293 cells transfected with TRP5 plus CD8 (*B* and *D*). In *A* and *B*, the perfusion solution was changed to Ca^{2+}-free HBS containing 0.5 mM EGTA, and 2 μM thapsigargin (TG) was applied to the cells in the absence of extracellular Ca^{2+}, which was followed by the addition of 2 mM extracellular Ca^{2+}. In *C* and *D*, the cells were treated with 2 μM thapsigargin in the presence of extracellular Ca^{2+}, then thapsigargin was replaced with 100 μM ATP. The duration of exposure to Ca^{2+}-containing HBS, Ca^{2+}-free HBS, 100 μM ATP, and 2 μM thapsigargin is indicated by the *filled*, *open*, *hatched*, and *shaded* bars, respectively, above the graphs. Data points are the means ± SEM $[Ca^{2+}]_i$ in the indicated number of cells.

Figure 7

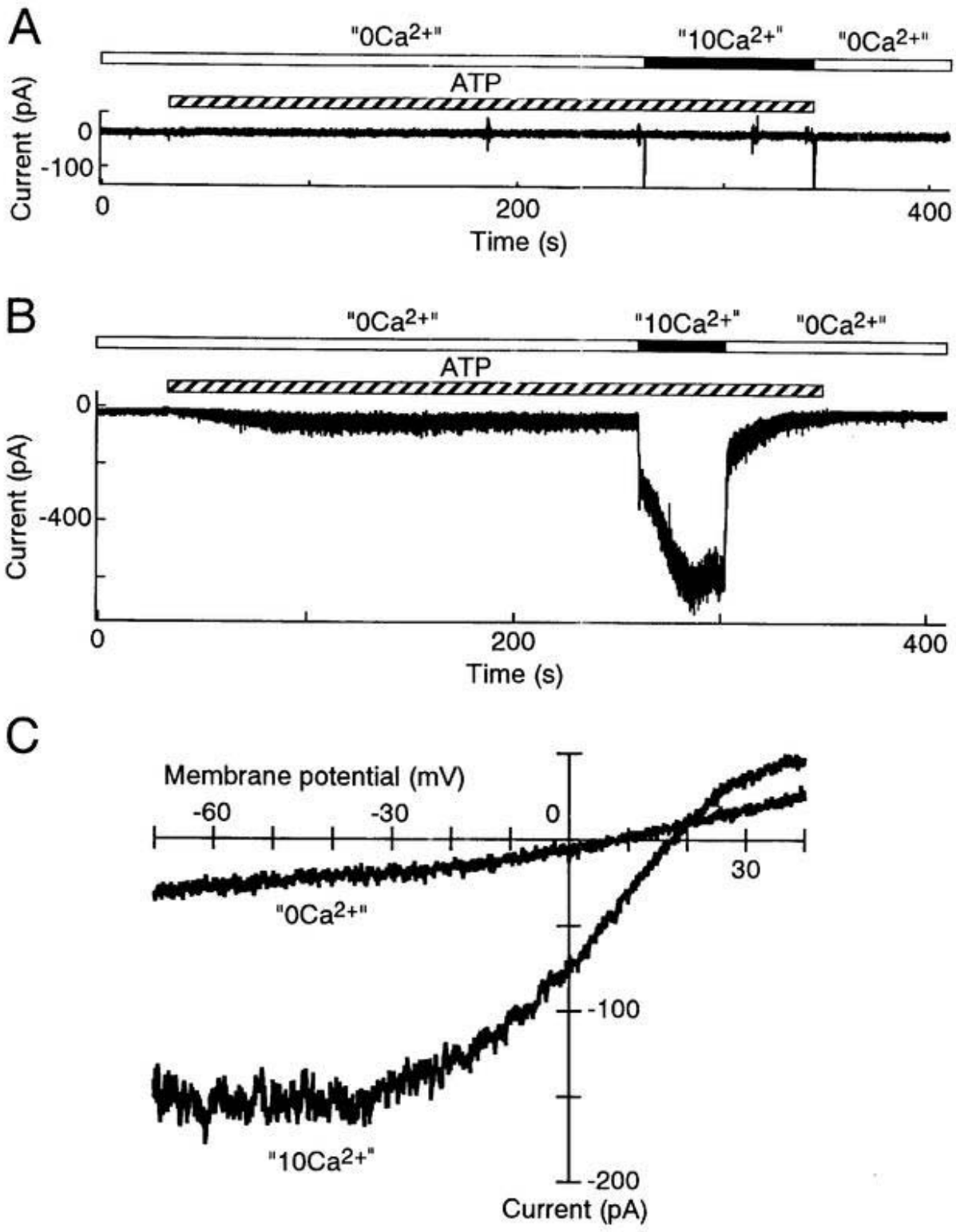
A
"0Ca2+"
"10Ca2+"
"0Ca2+"
ATP
Current (pA)
0
-100
0
200
400
Time (s)
B
"0Ca2+"
"10Ca2+"
"0Ca2+"
ATP
Current (pA)
0
-400
0
200
400
Time (s)
C
Membrane potential (mV)
-60
-30
0
30
"0Ca2+"
-100
"10Ca2+"
-200
Current (pA)

FIG. 7. **Electrophysiological characterization of the TRP5 channel.** In *A*, shown is a time course of ionic current recorded from a control HEK293 cell at a holding potential of -50 mV. During application of ATP (indicated by the *hatched bar* above the current) to the control HEK293 cell, the external solutions were changed from the "$0Ca^{2+}$" solution (*open bar*) to the "$10Ca^{2+}$" solution (*filled bar*). Finally, ATP was washed out with the "$0Ca^{2+}$" solution. In *B*, a time course of ionic current recorded from a HEK293 cell transfected with TRP5 plus CD8 is shown. In *C*, current-voltage relationships of the TRP5 channel are shown. Currents were evoked by 1.5 s negative voltage ramps from 40 to -70 mV. Five consecutive ramps were applied every 5 s in the "$0Ca^{2+}$" solution or the "$10Ca^{2+}$" solution with 100 μM ATP. The averaged currents were drawn. The currents shown in *B* and *C* were recorded from different TRP5-transfected cells.

Figure 8

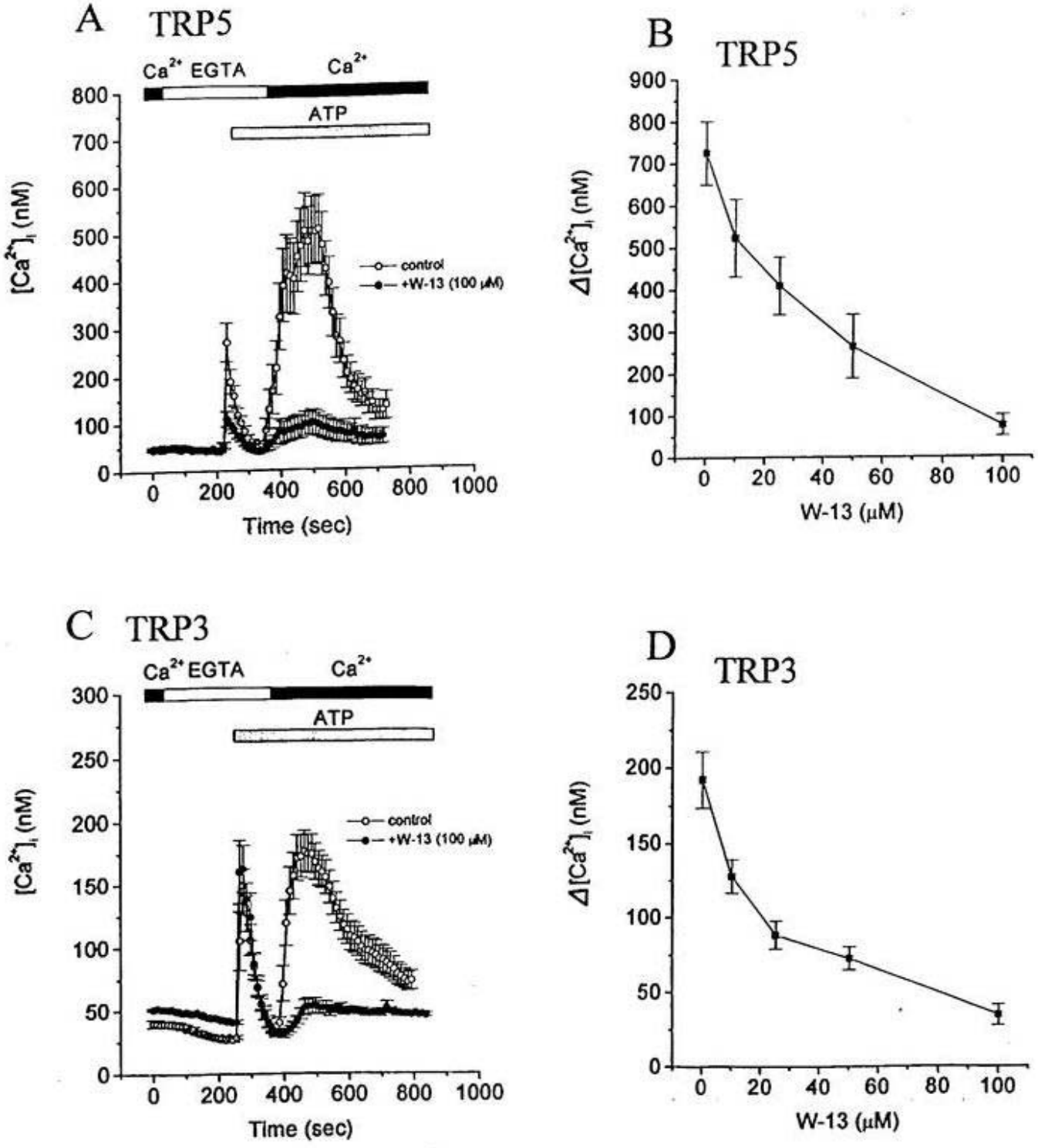
A
TRP5
Ca2+ EGTA
Ca2+
ATP
control
+W-13 (100 μM)
[Ca2+]i (nM)
Time (sec)
B
TRP5
Δ[Ca2+]i (nM)
W-13 (μM)
C
TRP3
Ca2+ EGTA
Ca2+
ATP
control
+W-13 (100 μM)
[Ca2+]i (nM)
Time (sec)
D
TRP3
Δ[Ca2+]i (nM)
W-13 (μM)

Fig. 8. **Inhibition of Ca^{2+} influx via TRP5 and TRP3 by calmodulin antagonist W-13.** Cytosolic Ca^{2+} was measured in fura-2-loaded TRP5- (*A* and *B*), and TRP3-transfected cells (*C* and *D*) in the presence of W-13 at various concentrations (0~100 μM). W-13 treatment started 4 min before the time 0 in *A* and *C*, and continued till the end of each experiment. The perfusion solution was changed to Ca^{2+}-free HBS, and 100 μM ATP was applied to the cells in the absence of extracellular Ca^{2+}, which was followed by the addition of 2 mM extracellular Ca^{2+}. In *A* and *C*, the time courses of $[Ca^{2+}]_i$ in the presence of 0 μM and 100 μM W-13 were shown representatively. The duration of exposure to Ca^{2+}-containing HBS, Ca^{2+}-free HBS, and 100 μM ATP is indicated by the *filled*, *open*, and *shaded bars*, respectively, above the graphs. In *B* and *D*, plotted is the amplitude of maximum $[Ca^{2+}]_i$ rises ($\Delta[Ca^{2+}]_i$) induced by the addition of 2 mM extracellular Ca^{2+} 2 min after the addition of ATP in individual cells against the concentration of W-13 used for treatment of the cells. Data points are the means ± SEM $[Ca^{2+}]_i$ or the means ± SEM $\Delta[Ca^{2+}]_i$ in 16-25 TRP5- or 21-32 TRP3-transfected cells.

Figure 9

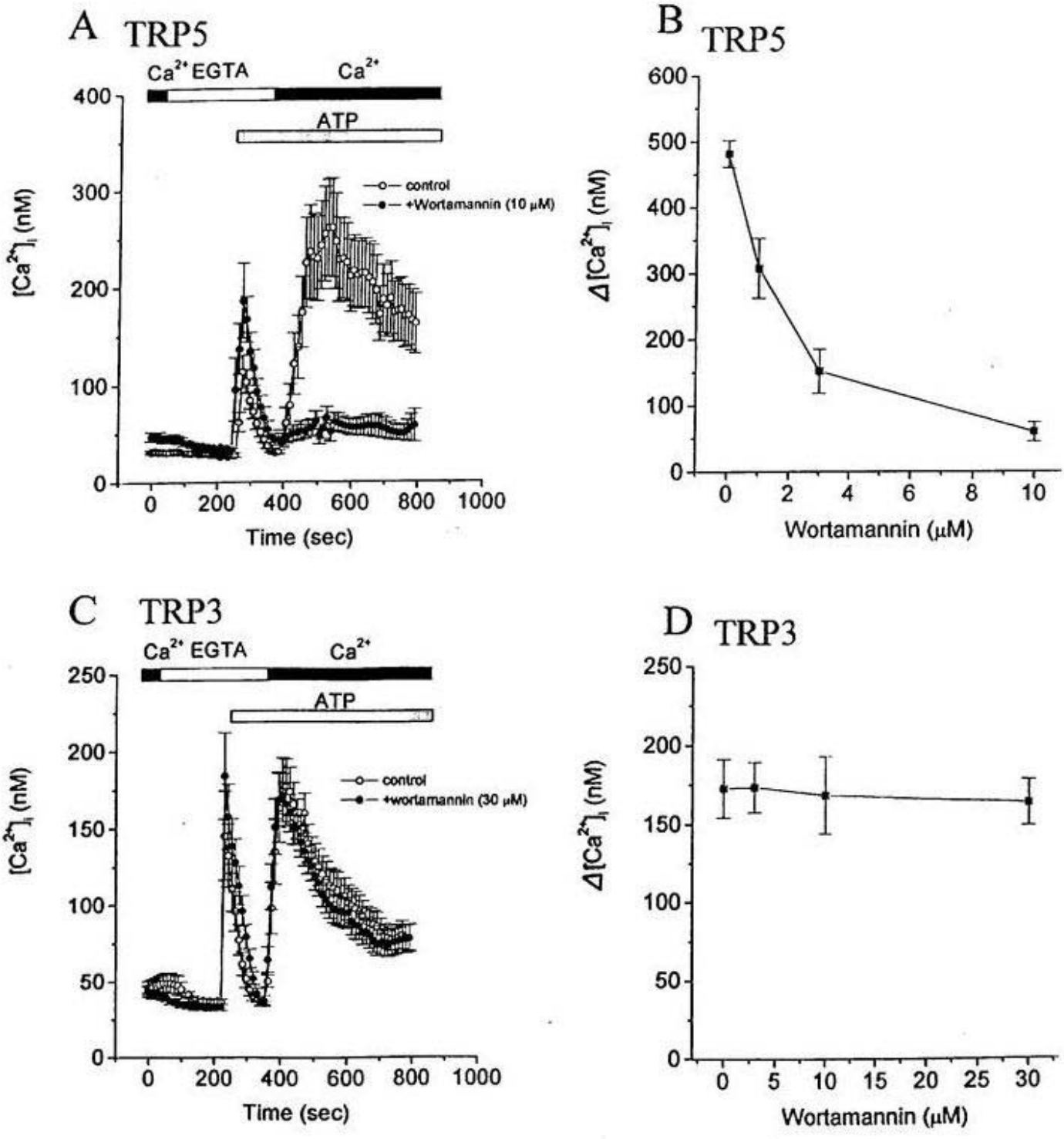
A TRP5
Ca2+ EGTA
Ca2+
ATP
control
+Wortamannin (10 μM)
[Ca2+]i (nM)
Time (sec)
B TRP5
Δ[Ca2+]i (nM)
Wortamannin (μM)
C TRP3
Ca2+ EGTA
Ca2+
ATP
control
+wortamannin (30 μM)
[Ca2+]i (nM)
Time (sec)
D TRP3
Δ[Ca2+]i (nM)
Wortamannin (μM)

Figure 9 continued

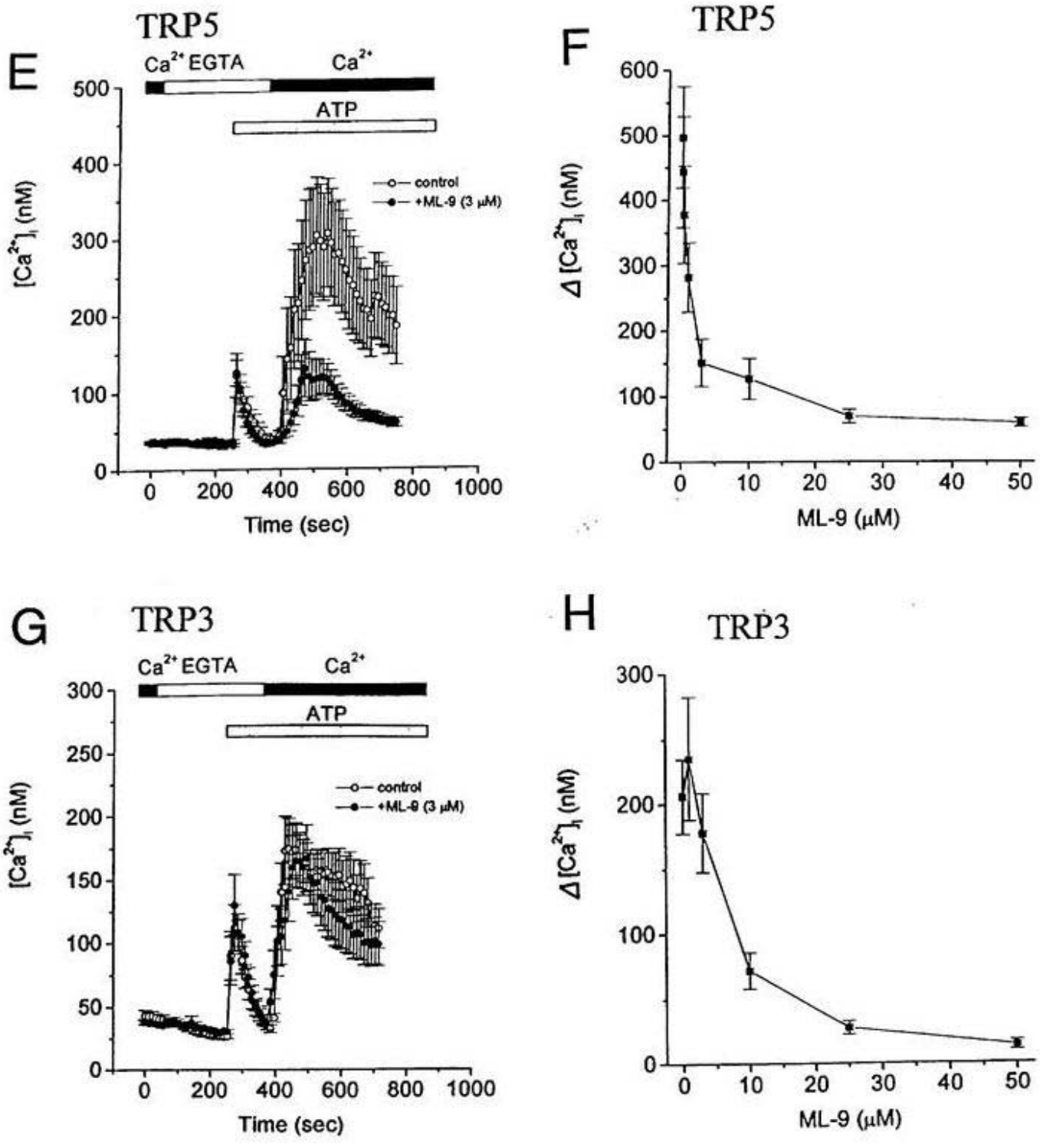

Fig. 9. **Inhibition of Ca^{2+} influx via TRP5 and TRP3 by MLCK inhibitors, Wortmannin and ML-9.** Cytosolic Ca^{2+} was measured in fura-2-loaded TRP5- (*A*, *B*, *E*, and *F*), and TRP3-transfected cells (*C*, *D*, *G*, and *H*) in the presence of Wortmannin (*A*~*D*) or ML-9 (*E*~*H*) at various concentrations. Treatment with Wortmannin started 30 min before the time 0 in *A* and *C*. Treatment with ML-9 started 4 min before the time 0 in *E* and *G*. Treatment continued till the end of each experiment. The perfusion solution was changed to Ca^{2+}-free HBS, and 100 μM ATP was applied to the cells in the absence of extracellular Ca^{2+}, which was followed by the addition of 2 mM extracellular Ca^{2+}. In *A* and *C*, the time courses of $[Ca^{2+}]_i$ in the presence of 0 μM and 10 μM Wortmannin, and in the presence of 0 μM and 30 μM Wortmannin, respectively, are shown representatively. In *E* and *G* the time courses of $[Ca^{2+}]_i$ in the presence of 0 μM and 3 μM ML-9 were shown representatively. The duration of exposure to Ca^{2+}-containing HBS, Ca^{2+}-free HBS, and 100 μM ATP is indicated by the *filled*, *open*, and *shaded bars*, respectively, above the graphs. In *B* and *D*, and *F* and *G*, plotted is the amplitude of maximum $[Ca^{2+}]_i$ rises ($\Delta[Ca^{2+}]_i$) induced by the addition of 2 mM extracellular Ca^{2+} 2 min after the addition of ATP in individual cells against the concentration of Wortmannin and ML-9, respectively, used for treatment of the cells. Data points are the means ± SEM $[Ca^{2+}]_i$ or the means ± SEM $\Delta[Ca^{2+}]_i$ in 23-29 TRP5- or 19-29 TRP3-transfected cells.

Figure 10

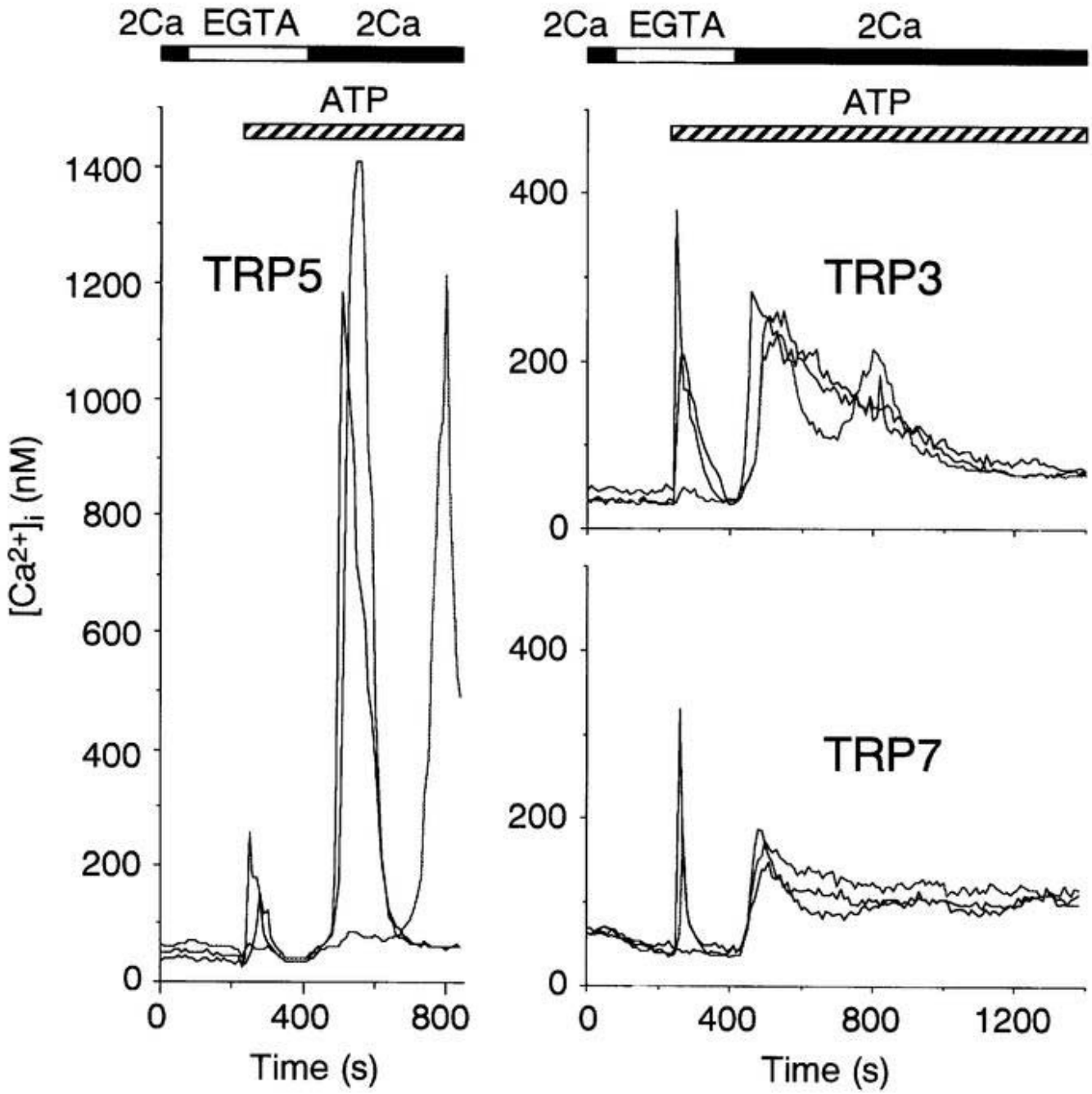
2Ca EGTA 2Ca
ATP
TRP5
TRP3
TRP7
[Ca2+]i (nM)
1400
1200
1000
800
600
400
200
0
0
400
800
1200
Time (s)

Fig. 10. **Typical examples of ATP-induced Ca^{2+} influx into individual TRP5-, TRP3-, and TRP7-expressing cells.** Shown are three typical examples of the time courses of $[Ca^{2+}]_i$ in individual TRP5-, TRP3-, or TRP7-transfected cells. The perfusion solution was first changed to Ca^{2+}-free HBS containing 0.5 mM EGTA, and 100 μM ATP was applied to the cells in the absence of extracellular Ca^{2+}. Three min after the application of ATP, 2 mM Ca^{2+} was further added to the extracellular solution. The duration of exposure to Ca^{2+}-containing HBS, Ca^{2+}-free HBS, and 100 μM ATP is indicated by the *filled*, *open*, and *hatched bars*, respectively, above the graphs.

Figure 11

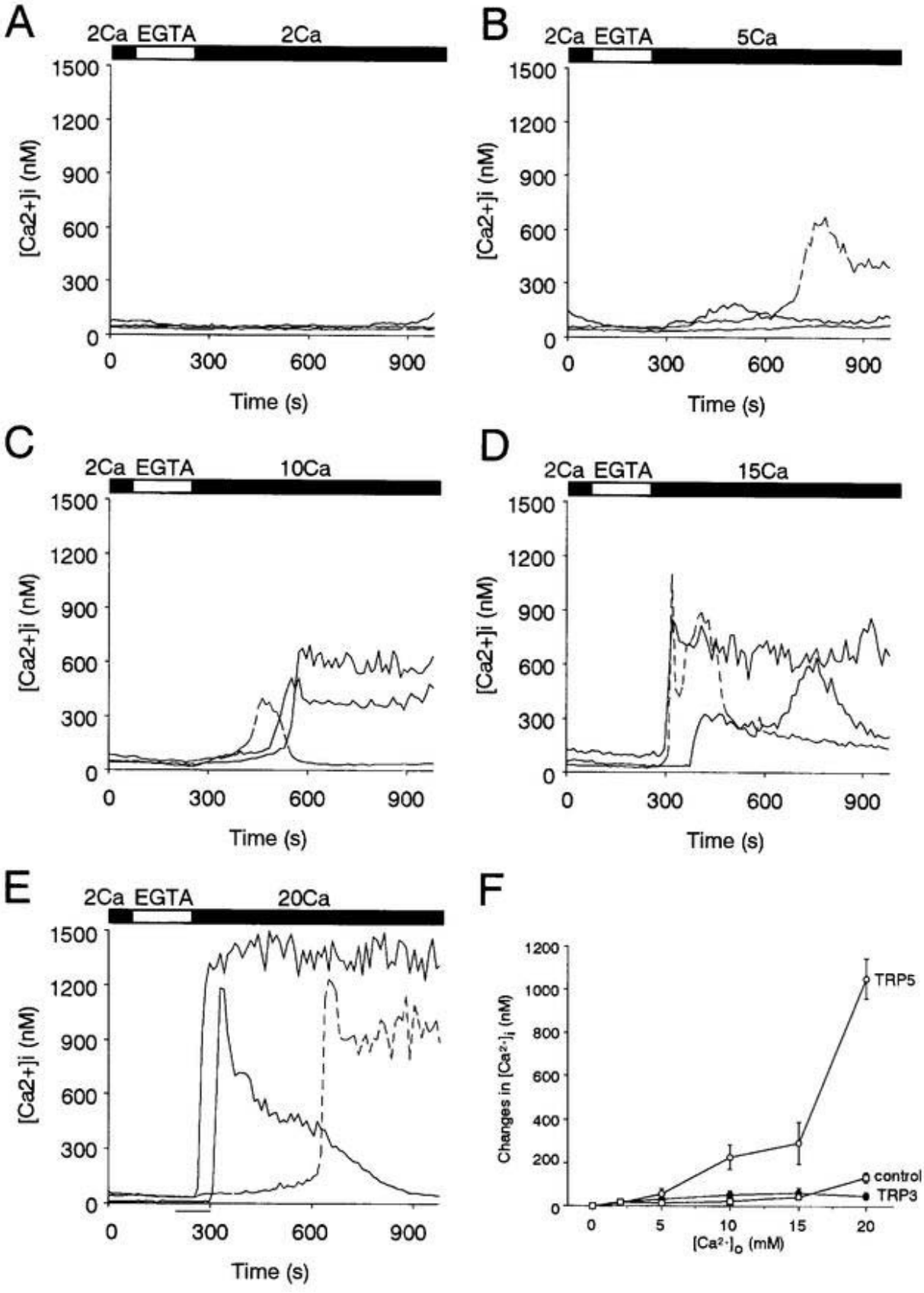
A
2Ca EGTA
2Ca
[Ca2+]i (nM)
Time (s)
B
2Ca EGTA
5Ca
C
2Ca EGTA
10Ca
D
2Ca EGTA
15Ca
E
2Ca EGTA
20Ca
F
Changes in [Ca2+]i (nM)
[Ca2+]o (mM)
TRP5
control
TRP3

Fig. 11. **$[Ca^{2+}]_i$ changes induced by raising extracellular Ca^{2+} in TRP5-, TRP3-, and vector-transfected HEK cells.** In *A*~*E*, typical examples of the time courses of $[Ca^{2+}]_i$ in indivisual TRP5-transfected cells are shown. The perfusion solution was first changed to Ca^{2+}-free HBS containing 0.5 mM EGTA, then to 2 mM (*A*), 5 mM (*B*), 10 mM (*C*), 15 mM (*D*), 20 mM (*E*) Ca^{2+}-containing HBS. The duration of exposure to Ca^{2+}-containing HBS and Ca^{2+}-free HBS is indicated by the *filled* and *open bars*, respectively, above the graphs. In *F*, plotted is the amplitude of maximum $[Ca^{2+}]_i$ rises ($\Delta[Ca^{2+}]_i$) induced by the addition of extracellular Ca^{2+} in indivisual TRP5- (*open circle*), TRP3- (*closed circle*), and vector-transfected cells (*open square*) against the concentration of extracellular Ca^{2+} added. Data points are the means ± SEM $\Delta[Ca^{2+}]_i$ in 18-28 TRP5-, 15-23 TRP3-, or 15-21 vector-transfected cells.

Figure 12

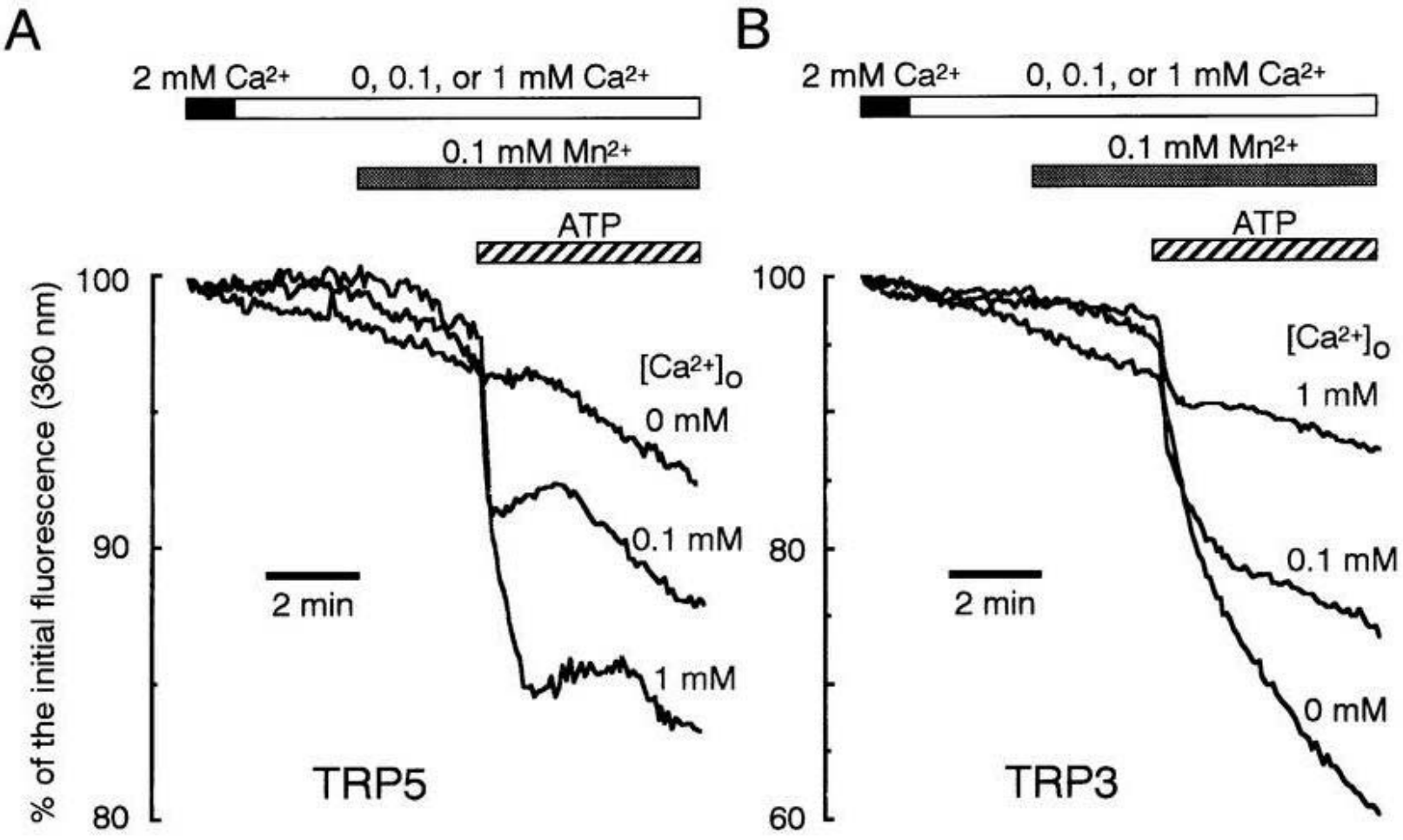
A
2 mM Ca2+
0, 0.1, or 1 mM Ca2+
0.1 mM Mn2+
ATP
100
90
80
% of the initial fluorescence (360 nm)
[Ca2+]o
0 mM
0.1 mM
1 mM
2 min
TRP5
B
2 mM Ca2+
0, 0.1, or 1 mM Ca2+
0.1 mM Mn2+
ATP
100
80
60
[Ca2+]o
1 mM
0.1 mM
0 mM
2 min
TRP3

Fig. 12. **ATP-induced Mn^{2+} influx in TRP5- and TRP3-transfected cells in the presence of extracellular Ca^{2+} at various concentrations.** Fluorescence quenching due to Mn^{2+} influx was observed by measuring fluorescence intensity at 510 nm of fura-2 excited at 360 nm in TRP5- (*A*) and TRP3-transfected cells (*B*). Perfusion solution was first changed to nominally Ca^{2+}-free, 0.1 mM Ca^{2+}-, or 1mM Ca^{2+}-containing HBS, and then 0.1 mM Mn^{2+} was added to the solution. Finally 100 μM ATP was further added to the solution. The duration of exposure to 2 mM Ca^{2+}-containing HBS is indicated by the *filled bars* above the graphs. The duration of nominally Ca^{2+}-free, 0.1 mM Ca^{2+}-containing, and 1 mM Ca^{2+}-containing HBS by the *open bars*. And the duration of exposure to 0.1 mM Mn^{2+} and 100 μM ATP by the *shaded* and *hatched bars*, respectively. The results are expressed as the mean ratios of fluorecence intensity to the initial value in 15~16 TRP5-, or 20~23 TRP3-transfected cells.

Figure 13

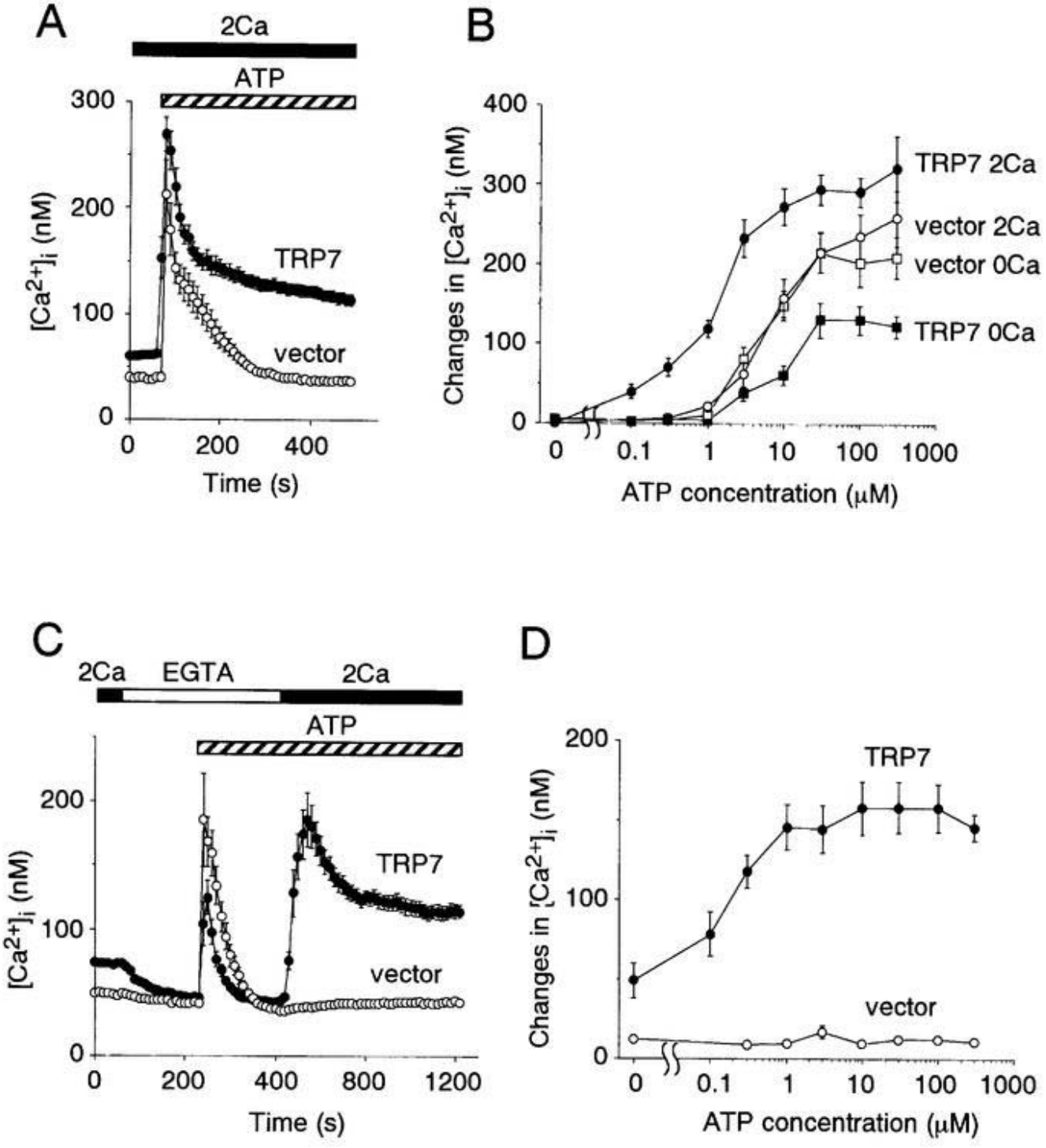
A
2Ca
ATP
300
200
100
0
$[Ca^{2+}]_i$ (nM)
TRP7
vector
0
200
400
Time (s)
B
400
300
200
100
0
Changes in $[Ca^{2+}]_i$ (nM)
TRP7 2Ca
vector 2Ca
vector 0Ca
TRP7 0Ca
0
0.1
1
10
100
1000
ATP concentration (μM)
C
2Ca
EGTA
2Ca
ATP
200
100
0
$[Ca^{2+}]_i$ (nM)
TRP7
vector
0
200
400
800
1200
Time (s)
D
200
100
0
Changes in $[Ca^{2+}]_i$ (nM)
TRP7
vector
0
0.1
1
10
100
1000
ATP concentration (μM)

Fig. 13. **ATP-induced $[Ca^{2+}]_i$ transients in TRP7- and vector-transfected HEK cells in the presence and absence of extracellular Ca^{2+}.** Cytosolic Ca^{2+} was measured in fura-2-loaded CD8 positive TRP7- and vector-transfected HEK293 cells. In *A*, the TRP7- (*closed circle*) and vector- (*open circle*) transfected cells were treated with 100 μM ATP in the presence of 2 mM extracellular Ca^{2+}. *B*, dose-response relationships for maximum ATP-induced $[Ca^{2+}]_i$ rises ($\Delta[Ca^{2+}]_i$) in individual TRP7- (*closed circle*) and vector- (*open circle*) transfected cells in the presence of 2 mM extracellular Ca^{2+}, and in TRP7- (*closed box*) and vector- (*open box*) transfected cells in the absence of extracellular Ca^{2+}. In *C*, the perfusion solution was changed to Ca^{2+}-free HBS, and 100 μM ATP was applied to the TRP7- (*closed circle*) and vector- (open circle) transfected cells in the absence of extracellular Ca^{2+}, which was followed by the addition of 2 mM extracellular Ca^{2+}. *D*, ATP concentration dependence of maximum $[Ca^{2+}]_i$ rises ($\Delta[Ca^{2+}]_i$) induced by the addition of 2 mM extracellular Ca^{2+} 3 min after the addition of ATP in individual TRP7- (*closed circle*) and vector- (*open circle*) transfected cells. The duration of exposure to Ca^{2+}-containing HBS, Ca^{2+}-free HBS and 100 μM ATP is indicated by the *filled*, *open*, and *hatched bars*, respectively, above the graphs. Data points are the means ± SEM $[Ca^{2+}]_i$ or the means ± SEM $\Delta[Ca^{2+}]_i$ in 29-40 TRP7- or 22-33 vector-transfected cells.

Figure 14

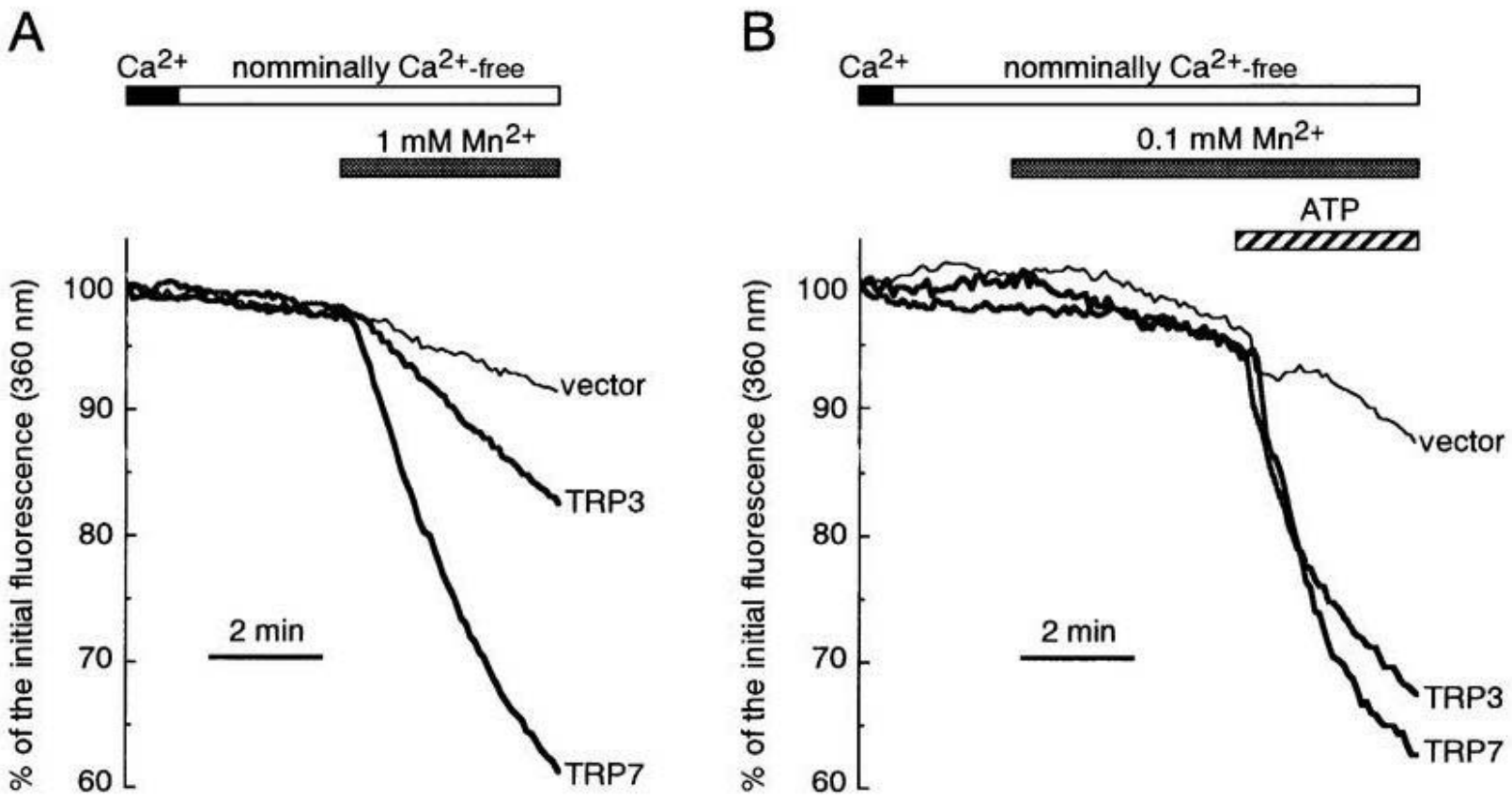
A
Ca2+
nomminally Ca2+-free
1 mM Mn2+
% of the initial fluorescence (360 nm)
100
90
80
70
60
2 min
vector
TRP3
TRP7
B
Ca2+
nomminally Ca2+-free
0.1 mM Mn2+
ATP
% of the initial fluorescence (360 nm)
100
90
80
70
60
2 min
vector
TRP3
TRP7

Fig. 14. **Basal and ATP-induced Mn^{2+} influx in TRP7-, TRP3-, and vector-transfected cells.** Fluorescence quenching due to Mn^{2+} influx was observed by measuring fluorescence intensity at 510 nm of fura-2 excited at 360 nm in TRP7- (*solid line*), TRP3- (*broken line*), and vector- (*dotted line*) transfected cells was measured. In *A*, perfusion solution was changed to nominally Ca^{2+}-free HBS without phosphate, and then 1 mM Mn^{2+} was added to the solution. In *B*, perfusion solution was changed to nominally Ca^{2+}-free HBS, and then 0.1 mM Mn^{2+} was added to the solution. Finally 100 μM ATP was added to the solution. The duration of exposure to Ca^{2+}-containing HBS, nominally Ca^{2+}-free HBS, Mn^{2+}, and 100 μM ATP is indicated by the *filled*, *open*, *shaded*, and *hatched bars*, respectively, above the graphs. The results are expressed as the mean ratios of fluorecence intensity to the initial value in 22 or 25 TRP7-, 21 or 27 TRP3-, and 17 or 24 vector-transfected cells.

ACKNOWLEDGMENT

I should like to express my sincere gratefulness to Professor Keiji Imoto, Department of Physiological Sciences, The Graduate University of Advanced Studies and Department of Information Physiology, National Institute for Physiological Sciences, for his guidance, encouragement and support during all these years.

Special gratitude goes to Dr. Yasuo Mori, Department of Physiological Sciences, The Graduate University of Advanced Studies and Department of Information Physiology, National Institute for Physiological Sciences, who showed me the essence of research work via supervising the present study.

I am also deeply grateful to Dr. Shunichi Shimizu, Dr. Minoru Wakamori, Dr. Naoyuki Takada and Dr. Junichi Nakai, Department of Information Physiology, National Institute for Physiological Sciences, Dr. Kazuto Yamazaki, Dr. Isao Tanaka and Dr. Kouhei Sawada, Tsukuba Research Laboratories Eisai Co., Ltd., Professor Tomohiro Kurosaki and Dr. Akito Maeda, Institute for Liver Research, Kansai Medical University, Professor Yasunobu Okada, Department of Correlative Physiology, National Institute for Physiological Sciences, Dr. Tohru Yamakuni, Mitsubishi Kasei Institute of Life Sciences, and Dr. Ryuji Inoue, Faculty of Medicine, Kyushu University, for their invaluable help and advice.

I would also like to express special thanks to Ms. Emiko Mori, Ms. Naomi Sekiguchi, Ms. Kumiko Saito, and all other members of our laboratory. Without their help, it would have been much more difficult to accomplish this work.

I appreciate Mr. Howard James Havens for his meaningful talking on the air, which diverted me when I worked alone at the laboratory late at night.

Many thanks to my parents, sisters, and Ms. Shizuko Okamoto, who have supported me to complete this thesis.

February 1999

Takaharu Okada